CONTINUUM EMISSION FROM ROTATING NON-GRAY STELLAR ATMOSPHERES. II

GEORGE W. COLLINS II
Perkins Observatory, The Ohio State and Ohio Weselyan Universities
Received May 14, 1966

ABSTRACT

In this paper we present the results of some calculations concerning the effects of rotation upon non-gray early-type stellar atmospheres. The results consist of forty-six spectral energy distributions for models having various masses, rotational velocities, and angles of inclination. The results are presented in the form of graphs of the monochromatic flux emitted by each model as well as tables of monochromatic magnitudes in units of wavelength and frequency, normalized to λ 5048. Additional tables contain the defining values of the models and the numerical value for the monochromatic flux at λ 5048. In addition, estimates of UBV colors and absolute magnitude M_v are given. The models considered include the same models for which Hβ line strengths have been calculated by Collins and Harrington.

The variation of the parameters, T_e and g, which define the local atmosphere structure, is also discussed. The results are critically compared with contemporary work in the field. The possible application of this material to rotational studies of stars in OB associations is considered. It is found that disentanglement of V_e and $V_e \sin i$ is not possible on the basis of continuum studies alone.

I. INTRODUCTION

This paper represents an extension of an earlier work (Collins 1965; cited herein as "Paper II"), wherein the approximation theory necessary to calculate the spectral energy distribution for a rotating star was developed. In this paper we shall present the results of extensive numerical calculations based on the theory developed in Paper II. Changes have been made which bring the assumptions concerning the properties of the stellar interior which affect the atmosphere (i.e., the total luminosity and polar radius) more into line with current theories of rotating stellar interiors. Some forty-six model atmospheres representing main-sequence stars having varying amounts of rotation and seen at various angles of inclination are presented. The initial non-rotating models are so chosen as to span the B-spectral class and should therefore be useful in investigating the effects of rotation on the upper main sequence. Monochromatic magnitudes of thirty-four wavelengths are presented along with the parameters necessary to specify the state of the atmosphere completely. In addition, UBV colors and M_v magnitudes have been estimated from the monochromatic fluxes. The results are critically compared with earlier work by the author (Collins 1963; cited herein as "Paper I") and that by Roxburgh and Strittmatter (1965), wherein the gray-atmosphere approximation was used.

Section II is devoted to a brief discussion of the calculation of the models and a study of the variation of the physical parameters T_e and g over the surface of the stars. The results are presented in normalized form so that they are applicable over the entire range of stars to which the interior studies of Roxburgh, Griffith, and Sweet (1965) apply. Section III contains a short description of material presented in graphical and tabular form. In the last section we compare results of the study with previous investigators and their application to some observational aspects of rotation.

II. CONSTRUCTION OF THE MODELS AND VARIATION OF PHYSICAL PARAMETERS WITH LATITUDE

The construction of the models presented in this paper closely parallels the theory previously developed in Paper II. However, modifications were made to include variations in the total luminosity and the polar radius due to rotation, indicated by the work

of Roxburgh *et al.* (1965) and Limber and Roberts (1965). The details of the methods required to take this variation into account are given in a recent paper by Collins and Harrington (1966). Indeed, the models presented here have the same defining parameters as the models presented in that work. Briefly, the equations which approximately represent the variation of luminosity and polar radius with rotation are

$$\begin{aligned} L(w) &= L(0)(1 - 0.1678\, w^2 - 0.0792\, w^4)\,, \\ R_p(w) &= R_p(0)\,(1 - 0.0540\, w^2 - 0.0547\, w^4)\,, \end{aligned} \tag{1}$$

where w is the fraction of the angular velocity at which the centrifugal forces just balance the gravitational forces on the equator of the star. These expressions differ from those used by Roxburgh and Strittmatter (1965) and thus lead to some qualitative differences in our results. We shall return to this point during a discussion of the results of the calculations.

It was felt that it would be useful to demonstrate how the parameters which determine the local emergent radiation field (T_e and g) vary over the surface of a rotating model. Such a variation is necessary if one wishes to estimate line strengths or other parameters that could be expected to influence the spectra of such a model. Under the assumption of a Roche-model gravitational potential and the von Zeipel law of gravity darkening, the variation of the effective temperature T_e and the local surface gravity are given by

$$T_e^4(w,0) = C(w)g_p(w), \qquad T_e^4(w,\theta) = T_e^4(w,0)g_n(w,\theta), \qquad g_p(w) = GM/R_p^2(w)\,. \tag{2}$$

The parameter $g_n(w,\theta)$ may be evaluated by means of equations (3) and (47) to be found in an earlier paper (Collins and Harrington 1966) but for convenience has been tabulated here in Table 1. Using the shape equations (eqs. [3], [4], and [6]) and equation (47) given by Collins and Harrington (1966) one may obtain the parameter $C(w)$. The parameter $\mathfrak{w}$ which appears in Table 1 represents the solution to equation (47) of Collins and Harrington (1966) and is required if one wishes to use the shape equations of Papers I and II directly. It is essentially an adjusted value of w brought about by the contraction of the polar radius with increasing angular velocity.

Perhaps the most convenient way of displaying the variation of the local surface gravity over the surface is to normalize it by the value for the non-rotating model. This allows not only the variation with latitude to be indicated but also intercomparisons of models having different values of w. Thus, we shall define a quantity

$$\mathfrak{g}_n(w,\theta) = g_\eta(w)g_n(w,\theta) = [R_p(0)/R(w,\theta)]^2\,, \tag{3}$$

where $g_\eta(w) = R_p^2(0)/R_p^2(w)$ and may also be found in Table 1. The variation of $\mathfrak{g}_n(w,\theta)$ with w and θ is shown in Figure 1, while the variation of the effective temperature is given in normalized form in Figure 2.

III. DESCRIPTION OF THE RESULTS

The primary results of this study are contained in Tables 2 and 3. While the meaning of most of the entries is self-explanatory, a word about their origin is indicated. Table 2 contains defining parameters, as well as those results which can be characterized by a single number for any given model. The first three quantities, M, w, and i, are the parameters required to specify the model and are the mass in solar units, fraction of angular breakup velocity, and angle of inclination, respectively. The next three quantities g_0, T_e (Polar), and F_ν represent parameters resulting from the calculations. The quantities g_0 and T_e (Polar) represent the polar surface gravity and effective temperatures for each model, respectively. The quantity F_ν is the absolute energy per unit solid angle radiated by the model at λ 5048. Since this is the wavelength to which all of the monochromatic magnitudes in Table 3 are referred, the quantity F_ν is used to recover the absolute

TABLE 1

Normalized Surface Gravity g_n

θ	g_η	1.000	1.035	1.123	1.194	1.259
	w	0.0	0.5	0.8	0.9	1.0
	$\mathcal{N}$	0.0	0.579	0.871	0.944	1.0
0°		1.000	1.000	1.000	1.000	1.000
10°		1.000	0.994	0.991	0.989	0.984
20°		1.000	0.977	0.950	0.941	0.935
30°		1.000	0.951	0.885	0.866	0.855
40°		1.000	0.917	0.802	0.768	0.747
50°		1.000	0.880	0.711	0.657	0.617
60°		1.000	0.843	0.620	0.538	0.470
70°		1.000	0.811	0.537	0.422	0.312
80°		1.000	0.786	0.473	0.317	0.153
90°		1.000	0.775	0.441	0.237	0.000

TABLE 2

Parameters M/M_o, w, and i Defining the Models and Calculated Parameters g_o, T_e (Polar), and F_v

Model	M/M_o	w	i^o	$g_o \times 10^4$	T_e (Polar)	$F_v \times 10^{20}$ (ergs/sec)	M_v	$(U-B)_o$	$(B-V)_o$
1	9	0	0	1.747	23328	11.988	-2.00	-0.91	-0.25
2	9	0.5	0	1.807	23754	12.811	-2.08	-0.91	-0.24
3			45	1.807	23754	12.154	-2.02	-0.90	-0.24
4			90	1.807	23754	11.581	-1.97	-0.88	-0.24
5	9	0.8	0	1.964	24640	14.500	-2.21	-0.89	-0.24
6			45	1.964	24640	12.464	-2.05	-0.88	-0.23
7			90	1.964	24640	10.565	-1.87	-0.84	-0.22
8	9	0.9	0	2.062	25074	15.667	-2.30	-0.88	-0.24
9			45	2.062	25074	12.624	-2.06	-0.86	-0.23
10			90	2.062	25074	9.832	-1.79	-0.81	-0.21
11	9	1.0	0	2.199	25759	18.154	-2.45	-0.85	-0.23
12			45	2.199	25759	12.754	-2.07	-0.84	-0.22
13			90	2.199	25759	8.122	-1.58	-0.75	-0.19
14	6	0	0	1.860	18425	4.976	-1.05	-0.70	-0.19
15	6	0.5	0	1.924	18761	5.328	-1.13	-0.69	-0.19
16			45	1.924	18761	5.059	-1.07	-0.68	-0.19
17			57	1.924	18761	4.961	-1.05	-0.67	-0.19
18			90	1.924	18761	4.827	-1.02	-0.66	-0.19
19	6	0.8	0	2.091	19403	6.034	-1.26	-0.68	-0.19
20			45	2.091	19403	5.176	-1.09	-0.65	-0.19
21			57	2.091	19403	4.830	-1.02	-0.64	-0.18
22			90	2.091	19403	4.378	-0.91	-0.62	-0.17
23	6	0.9	0	2.196	19836	6.504	1.34	-0.67	-0.19
24			15	2.196	19836	6.289	-1.31	-0.67	-0.19
25			30	2.196	19836	5.840	-1.23	-0.65	-0.19
26			45	2.196	19836	5.217	-1.10	-0.64	-0.18
27			57	2.196	19836	4.709	-0.99	-0.62	-0.17
28			90	2.196	19836	4.043	-0.83	-0.57	-0.16
29	6	1.0	0	2.341	20348	7.310	-1.47	-0.61	-0.17
30			45	2.341	20348	5.113	-1.08	-0.59	-0.16
31			57	2.341	20348	4.247	-0.88	-0.56	-0.15
32			90	2.341	20348	3.154	-0.56	-0.48	-0.11
33	5	0	0	1.910	16457	3.326	-0.61	-0.59	-0.17
34	5	0.5	0	1.977	16758	3.567	-0.69	-0.59	-0.17
35			45	1.977	16758	3.385	-0.63	-0.57	-0.17
36			90	1.977	16758	3.231	-0.58	-0.56	-0.17
37	5	0.8	0	2.148	17327	4.009	-0.82	-0.57	-0.17
38			45	2.148	17327	3.428	-0.65	-0.54	-0.16
39			90	2.148	17327	2.885	-0.44	-0.49	-0.15
40	5	0.9	0	2.255	17687	4.291	-0.89	-0.56	-0.16
41			45	2.255	17687	3.424	-0.65	-0.51	-0.15
42			90	2.255	17687	2.624	-0.36	-0.43	-0.12
43	5	1.0	0	2.404	18173	4.674	-0.98	-0.47	-0.13
44			45	2.405	18173	3.260	-0.59	-0.43	-0.12
45			90	2.405	18173	1.936	-0.02	-0.27	-0.04
46	4	0	0	1.968	14169	1.948	-0.03	-0.42	-0.13
47	7.5	0	0	6.410	20000	21.240	-2.63	-0.80	-0.21
48	5	0	0	4.273	20000	21.400	-2.64	-0.81	-0.21
49	2.5	0	0	2.137	20000	21.670	-2.65	-0.85	-0.20

TABLE 3

Monochromatic Magnitude Relative to λ5040

	Model No. 1		Model No. 2		Model No. 3		Model No. 4		Model No. 5		
λ(Å)	M(1/λ)	M(λ)	M(1/λ)	M(λ)	M(1/λ)	M(λ)	M(1/λ)	M(λ)	M(1/λ)	M(λ)	$1/\lambda(\mu^{-1})$
58350.0	+ 4.84	+10.16	+ 4.84	+10.15	+ 4.83	+10.14	+ 4.81	+10.13	+ 4.83	+10.15	0.171
29180.0	+ 3.36	+ 7.17	+ 3.36	+ 7.17	+ 3.35	+ 7.16	+ 3.34	+ 7.15	+ 3.35	+ 7.16	0.343
19450.0	+ 2.51	+ 5.44	+ 2.51	+ 5.44	+ 2.50	+ 5.43	+ 2.49	+ 5.42	+ 2.50	+ 5.43	0.514
14590.0	+ 1.91	+ 4.21	+ 1.90	+ 4.21	+ 1.90	+ 4.20	+ 1.88	+ 4.19	+ 1.90	+ 4.20	0.685
14590.0	+ 1.94	+ 4.24	+ 1.93	+ 4.24	+ 1.93	+ 4.23	+ 1.92	+ 4.22	+ 1.93	+ 4.23	0.685
12210.0	+ 1.57	+ 3.49	+ 1.57	+ 3.49	+ 1.56	+ 3.48	+ 1.55	+ 3.47	+ 1.56	+ 3.48	0.819
10500.0	+ 1.27	+ 2.86	+ 1.27	+ 2.86	+ 1.26	+ 2.85	+ 1.25	+ 2.84	+ 1.26	+ 2.85	0.952
9214.0	+ 1.01	+ 2.32	+ 1.01	+ 2.32	+ 1.01	+ 2.31	+ 1.00	+ 2.30	+ 1.01	+ 2.31	1.085
8206.0	+ 0.78	+ 1.84	+ 0.78	+ 1.84	+ 0.78	+ 1.83	+ 0.77	+ 1.83	+ 0.78	+ 1.83	1.219
8206.0	+ 0.88	+ 1.93	+ 0.88	+ 1.93	+ 0.87	+ 1.93	+ 0.87	+ 1.92	+ 0.87	+ 1.93	1.219
6251.0	+ 0.38	+ 0.84	+ 0.38	+ 0.84	+ 0.37	+ 0.84	+ 0.37	+ 0.84	+ 0.37	+ 0.84	1.600
5048.0	0.00	0.00	0.00	0.00	0.00	0.00	0.00	0.00	0.00	0.00	1.981
4234.0	- 0.30	- 0.68	- 0.30	- 0.68	- 0.29	- 0.68	- 0.29	- 0.67	- 0.29	- 0.68	2.362
3646.0	- 0.51	- 1.22	- 0.51	- 1.21	- 0.50	- 1.21	- 0.50	- 1.20	- 0.50	- 1.21	2.743
3646.0	- 0.06	- 0.76	- 0.05	- 0.75	- 0.04	- 0.74	- 0.02	- 0.73	- 0.03	- 0.74	2.743
2652.0	- 0.42	- 1.82	- 0.40	- 1.80	- 0.39	- 1.78	- 0.36	- 1.76	- 0.39	- 1.79	3.771
2083.0	- 0.66	- 2.58	- 0.65	- 2.57	- 0.62	- 2.54	- 0.58	- 2.51	- 0.63	- 2.55	4.801
1716.0	- 0.83	- 3.18	- 0.82	- 3.16	- 0.78	- 3.13	- 0.74	- 3.08	- 0.81	- 3.15	5.828
1458.0	- 0.97	- 3.67	- 0.95	- 3.65	- 0.91	- 3.61	- 0.86	- 3.55	- 0.95	- 3.64	6.859
1458.0	- 0.97	- 3.67	- 0.95	- 3.65	- 0.91	- 3.61	- 0.86	- 3.55	- 0.95	- 3.64	6.859
1268.0	- 1.07	- 4.07	- 1.05	- 4.05	- 1.00	- 4.00	- 0.94	- 3.94	- 1.05	- 4.05	7.886
1122.0	- 1.15	- 4.41	- 1.13	- 4.39	- 1.07	- 4.34	- 1.01	- 4.27	- 1.12	- 4.39	8.913
1006.0	- 1.21	- 4.71	- 1.19	- 4.69	- 1.13	- 4.63	- 1.06	- 4.56	- 1.18	- 4.68	9.940
911.6	- 1.24	- 4.95	- 1.21	- 4.93	- 1.15	- 4.87	- 1.08	- 4.79	- 1.20	- 4.92	10.970
911.6	+ 5.27	+ 1.55	+ 5.51	+ 1.80	+ 5.68	+ 1.96	+ 5.91	+ 2.19	+ 5.64	+ 1.93	10.970
758.7	+ 6.91	+ 2.80	+ 7.20	+ 3.09	+ 7.41	+ 3.29	+ 7.71	+ 3.59	+ 7.33	+ 3.22	13.180
649.4	+ 8.61	+ 4.15	+ 8.92	+ 4.47	+ 9.16	+ 4.70	+ 9.53	+ 5.07	+ 9.05	+ 4.60	15.399
567.8	+10.32	+ 5.58	+10.65	+ 5.90	+10.91	+ 6.17	+11.34	+ 6.60	+10.77	+ 6.03	17.612
504.3	+12.05	+ 7.05	+12.38	+ 7.38	+12.66	+ 7.66	+13.14	+ 8.14	+12.49	+ 7.48	19.829
504.3	+12.21	+ 7.20	+12.57	+ 7.57	+12.83	+ 7.83	+13.27	+ 8.26	+12.72	+ 7.71	19.829
387.0	+17.20	+11.62	+17.58	+12.00	+17.86	+12.28	+18.33	+12.75	+17.73	+12.15	25.840
314.0	+22.34	+16.31	+22.73	+16.70	+23.01	+16.98	+23.49	+17.46	+22.88	+16.85	31.847
264.1	+27.61	+21.20	+28.00	+21.59	+28.28	+21.87	+28.77	+22.36	+28.14	+21.74	37.864
228.0	+32.94	+26.21	+33.32	+26.59	+33.61	+26.88	+34.09	+27.37	+33.47	+26.74	43.860

TABLE 3 -- Continued

	Model No. 6		Model No. 7		Model No. 8		Model No. 9		Model No. 10		
λ(Å)	M(1/λ)	M(λ)	M(1/λ)	M(λ)	M(1/λ)	M(λ)	M(1/λ)	M(λ)	M(1/λ)	M(λ)	$1/\lambda(\mu^{-1})$
58350.0	+ 4.80	+10.12	+ 4.75	+10.07	+ 4.82	+10.14	+ 4.78	+10.10	+ 4.70	+10.01	0.171
29180.0	+ 3.32	+ 7.13	+ 3.28	+ 7.09	+ 3.34	+ 7.15	+ 3.30	+ 7.11	+ 3.23	+ 7.04	0.343
19450.0	+ 2.48	+ 5.40	+ 2.44	+ 5.37	+ 2.49	+ 5.42	+ 2.46	+ 5.39	+ 2.39	+ 5.32	0.514
14590.0	+ 1.88	+ 4.18	+ 1.84	+ 4.15	+ 1.89	+ 4.19	+ 1.86	+ 4.17	+ 1.80	+ 4.11	0.685
14590.0	+ 1.91	+ 4.21	+ 1.87	+ 4.18	+ 1.92	+ 4.23	+ 1.89	+ 4.20	+ 1.84	+ 4.14	0.685
12210.0	+ 1.55	+ 3.46	+ 1.52	+ 3.44	+ 1.56	+ 3.47	+ 1.53	+ 3.45	+ 1.48	+ 3.40	0.819
10500.0	+ 1.25	+ 2.84	+ 1.22	+ 2.81	+ 1.26	+ 2.85	+ 1.24	+ 2.83	+ 1.19	+ 2.78	0.952
9214.0	+ 0.99	+ 2.30	+ 0.97	+ 2.27	+ 1.00	+ 2.31	+ 0.98	+ 2.29	+ 0.94	+ 2.25	1.085
8206.0	+ 0.77	+ 1.82	+ 0.74	+ 1.80	+ 0.77	+ 1.83	+ 0.76	+ 1.81	+ 0.72	+ 1.78	1.219
8206.0	+ 0.86	+ 1.92	+ 0.85	+ 1.90	+ 0.87	+ 1.93	+ 0.86	+ 1.91	+ 0.83	+ 1.88	1.219
6251.0	+ 0.37	+ 0.83	+ 0.36	+ 0.83	+ 0.37	+ 0.84	+ 0.37	+ 0.83	+ 0.35	+ 0.82	1.600
5048.0	0.00	0.00	0.00	0.00	0.00	0.00	0.00	0.00	0.00	0.00	1.981
4234.0	- 0.29	- 0.67	- 0.28	- 0.66	- 0.29	- 0.68	- 0.29	- 0.67	- 0.27	- 0.65	2.362
3646.0	- 0.49	- 1.20	- 0.48	- 1.18	- 0.50	- 1.21	- 0.49	- 1.20	- 0.46	- 1.17	2.743
3646.0	- 0.01	- 0.72	+ 0.03	- 0.67	- 0.03	- 0.73	0.00	- 0.70	+ 0.07	- 0.63	2.743
2652.0	- 0.35	- 1.75	- 0.28	- 1.68	- 0.38	- 1.78	- 0.33	- 1.73	- 0.21	- 1.61	3.771
2083.0	- 0.58	- 2.50	- 0.48	- 2.40	- 0.63	- 2.55	- 0.55	- 2.47	- 0.38	- 2.30	4.801
1716.0	- 0.74	- 3.08	- 0.61	- 2.95	- 0.80	- 3.15	- 0.71	- 3.05	- 0.49	- 2.83	5.828
1458.0	- 0.86	- 3.56	- 0.70	- 3.40	- 0.95	- 3.64	- 0.83	- 3.53	- 0.56	- 3.26	6.859
1458.0	- 0.86	- 3.56	- 0.70	- 3.40	- 0.95	- 3.64	- 0.83	- 3.53	- 0.56	- 3.26	6.859
1268.0	- 0.95	- 3.95	- 0.77	- 3.77	- 1.05	- 4.05	- 0.92	- 3.92	- 0.61	- 3.61	7.886
1122.0	- 1.01	- 4.28	- 0.81	- 4.08	- 1.12	- 4.39	- 0.98	- 4.24	- 0.63	- 3.90	8.913
1006.0	- 1.06	- 4.56	- 0.84	- 4.34	- 1.18	- 4.68	- 1.02	- 4.53	- 0.65	- 4.15	9.940
911.6	- 1.08	- 4.79	- 0.84	- 4.56	- 1.20	- 4.92	- 1.04	- 4.75	- 0.63	- 4.34	10.970
911.6	+ 5.78	+ 2.07	+ 6.25	+ 2.53	+ 5.59	+ 1.87	+ 5.71	+ 1.99	+ 6.29	+ 2.57	10.970
758.7	+ 7.51	+ 3.39	+ 8.11	+ 4.00	+ 7.25	+ 3.13	+ 7.38	+ 3.27	+ 8.09	+ 3.98	13.180
649.4	+ 9.25	+ 4.80	+ 9.99	+ 5.35	+ 8.94	+ 4.48	+ 9.09	+ 4.64	+ 9.91	+ 5.45	15.399
567.8	+10.99	+ 6.25	+11.85	+ 7.10	+10.63	+ 5.89	+10.80	+ 6.06	+11.71	+ 6.96	17.612
504.3	+12.74	+ 7.73	+13.69	+ 8.68	+12.33	+ 7.33	+12.53	+ 7.52	+13.51	+ 8.51	19.829
504.3	+12.92	+ 7.91	+13.77	+ 8.77	+12.58	+ 7.58	+12.72	+ 7.72	+13.59	+ 8.59	19.829
387.0	+17.94	+12.36	+18.87	+13.29	+17.58	+12.00	+17.72	+12.14	+18.64	+13.06	25.840
314.0	+23.09	+17.06	+24.04	+18.01	+22.73	+16.70	+22.87	+16.84	+23.80	+17.77	31.847
264.1	+28.36	+21.95	+29.32	+22.91	+27.99	+21.58	+28.14	+21.73	+29.07	+22.66	37.864
228.0	+33.68	+26.96	+34.65	+27.92	+33.31	+26.59	+33.46	+26.73	+34.40	+27.67	43.860

TABLE 3 -- Continued

	Model No. 11		Model No. 12		Model No. 13		Model No. 14		Model No. 15		
λ(Å)	M(1/λ)	M(λ)	M(1/λ)	M(λ)	M(1/λ)	M(λ)	M(1/λ)	M(λ)	M(1/λ)	M(λ)	1/λ(μ^{-1})
58350.0	+ 4.76	+10.08	+ 4.73	+10.04	+ 4.57	+ 9.89	+ 4.62	+ 9.94	+ 4.62	+ 9.93	0.171
29180.0	+ 3.29	+ 7.10	+ 3.26	+ 7.07	+ 3.12	+ 6.93	+ 3.16	+ 6.97	+ 3.15	+ 6.96	0.343
19450.0	+ 2.44	+ 5.37	+ 2.42	+ 5.35	+ 2.30	+ 5.23	+ 2.33	+ 5.25	+ 2.32	+ 5.25	0.514
14590.0	+ 1.85	+ 4.15	+ 1.83	+ 4.13	+ 1.72	+ 4.03	+ 1.74	+ 4.05	+ 1.74	+ 4.04	0.685
14590.0	+ 1.88	+ 4.19	+ 1.86	+ 4.17	+ 1.76	+ 4.06	+ 1.78	+ 4.08	+ 1.77	+ 4.08	0.685
12210.0	+ 1.52	+ 3.44	+ 1.51	+ 3.42	+ 1.41	+ 3.33	+ 1.43	+ 3.35	+ 1.43	+ 3.35	0.819
10500.0	+ 1.23	+ 2.82	+ 1.21	+ 2.80	+ 1.13	+ 2.72	+ 1.14	+ 2.73	+ 1.14	+ 2.73	0.952
9214.0	+ 0.97	+ 2.28	+ 0.96	+ 2.26	+ 0.88	+ 2.19	+ 0.89	+ 2.20	+ 0.89	+ 2.20	1.085
8206.0	+ 0.75	+ 1.80	+ 0.74	+ 1.79	+ 0.67	+ 1.73	+ 0.68	+ 1.74	+ 0.68	+ 1.73	1.219
8206.0	+ 0.86	+ 1.91	+ 0.84	+ 1.90	+ 0.79	+ 1.84	+ 0.81	+ 1.86	+ 0.80	+ 1.86	1.219
6251.0	+ 0.36	+ 0.83	+ 0.36	+ 0.82	+ 0.33	+ 0.80	+ 0.34	+ 0.81	+ 0.34	+ 0.80	1.600
5048.0	0.00	0.00	0.00	0.00	0.00	0.00	0.00	0.00	0.00	0.00	1.981
4234.0	- 0.29	- 0.67	- 0.28	- 0.66	- 0.26	- 0.64	- 0.26	- 0.64	- 0.26	- 0.64	2.362
3646.0	- 0.49	- 1.20	- 0.48	- 1.19	- 0.44	- 1.14	- 0.45	- 1.15	- 0.45	- 1.15	2.743
3646.0	+ 0.02	- 0.69	+ 0.04	- 0.67	+ 0.14	- 0.56	+ 0.20	- 0.50	+ 0.21	- 0.50	2.743
2652.0	- 0.33	- 1.72	- 0.29	- 1.69	- 0.09	- 1.49	- 0.03	- 1.43	- 0.02	- 1.42	3.771
2083.0	- 0.57	- 2.49	- 0.51	- 2.43	- 0.23	- 2.15	- 0.17	- 2.09	- 0.16	- 2.08	4.801
1716.0	- 0.74	- 3.09	- 0.67	- 3.02	- 0.31	- 2.66	- 0.26	- 2.60	- 0.25	- 2.59	5.828
1458.0	- 0.88	- 3.58	- 0.79	- 3.49	- 0.37	- 3.06	- 0.32	- 3.02	- 0.30	- 3.00	6.859
1458.0	- 0.88	- 3.58	- 0.79	- 3.49	- 0.37	- 3.06	- 0.32	- 3.02	- 0.30	- 3.00	6.859
1268.0	- 0.98	- 3.98	- 0.88	- 3.88	- 0.40	- 3.40	- 0.35	- 3.35	- 0.34	- 3.34	7.886
1122.0	- 1.06	- 4.32	- 0.94	- 4.21	- 0.41	- 3.67	- 0.38	- 3.64	- 0.36	- 3.62	8.913
1006.0	- 1.11	- 4.61	- 0.99	- 4.49	- 0.41	- 3.91	- 0.39	- 3.89	- 0.37	- 3.87	9.940
911.6	- 1.13	- 4.85	- 1.00	- 4.71	- 0.38	- 4.09	- 0.33	- 4.05	- 0.34	- 4.06	10.970
911.6	+ 5.60	+ 1.88	+ 5.60	+ 1.88	+ 6.14	+ 2.42	+ 7.95	+ 4.23	+ 8.15	+ 4.43	10.970
758.7	+ 7.23	+ 3.11	+ 7.23	+ 3.12	+ 7.87	+ 3.75	+10.27	+ 6.16	+10.54	+ 6.43	13.180
649.4	+ 8.89	+ 4.44	+ 8.91	+ 4.45	+ 9.62	+ 5.16	+12.64	+ 8.19	+12.97	+ 8.52	15.399
567.8	+10.57	+ 5.82	+10.60	+ 5.86	+11.38	+ 6.63	+15.03	+10.29	+15.41	+10.67	17.612
504.3	+12.25	+ 7.24	+12.30	+ 7.30	+13.15	+ 8.15	+17.44	+12.43	+17.85	+12.85	19.829
504.3	+12.53	+ 7.52	+12.52	+ 7.52	+13.24	+ 8.23	+17.47	+12.47	+17.90	+12.89	19.829
387.0	+17.52	+11.94	+17.51	+11.93	+18.25	+12.67	+24.11	+18.54	+24.61	+19.03	25.840
314.0	+22.66	+16.63	+22.65	+16.62	+23.40	+17.37	+30.87	+24.84	+31.38	+25.35	31.847
264.1	+27.92	+21.51	+27.92	+21.51	+28.67	+22.27	+37.73	+31.32	+38.25	+31.84	37.864
228.0	+33.24	+26.52	+33.24	+26.52	+34.00	+27.28	+44.64	+37.91	+45.15	+38.43	43.860

TABLE 3 -- Continued

	Model No. 16		Model No. 17		Model No. 18		Model No. 19		Model No. 20		
λ(Å)	M(1/λ)	M(λ)	M(1/λ)	M(λ)	M(1/λ)	M(λ)	M(1/λ)	M(λ)	M(1/λ)	M(λ)	$1/\lambda(\mu^{-1})$
58350.0	+ 4.60	+ 9.92	+ 4.60	+ 9.91	+ 4.58	+ 9.90	+ 4.60	+ 9.91	+ 4.56	+ 9.88	0.171
29180.0	+ 3.14	+ 6.95	+ 3.13	+ 6.94	+ 3.12	+ 6.93	+ 3.14	+ 6.95	+ 3.10	+ 6.91	0.343
19450.0	+ 2.31	+ 5.24	+ 2.30	+ 5.23	+ 2.29	+ 5.22	+ 2.31	+ 5.24	+ 2.28	+ 5.21	0.514
14590.0	+ 1.73	+ 4.03	+ 1.72	+ 4.03	+ 1.72	+ 4.02	+ 1.73	+ 4.03	+ 1.70	+ 4.01	0.685
14590.0	+ 1.76	+ 4.07	+ 1.76	+ 4.06	+ 1.75	+ 4.06	+ 1.76	+ 4.07	+ 1.74	+ 4.04	0.685
12210.0	+ 1.42	+ 3.34	+ 1.41	+ 3.33	+ 1.41	+ 3.33	+ 1.42	+ 3.34	+ 1.40	+ 3.32	0.819
10500.0	+ 1.13	+ 2.72	+ 1.13	+ 2.72	+ 1.12	+ 2.71	+ 1.13	+ 2.72	+ 1.11	+ 2.70	0.952
9214.0	+ 0.88	+ 2.19	+ 0.88	+ 2.19	+ 0.88	+ 2.18	+ 0.88	+ 2.19	+ 0.87	+ 2.17	1.085
8206.0	+ 0.67	+ 1.73	+ 0.67	+ 1.72	+ 0.66	+ 1.72	+ 0.67	+ 1.73	+ 0.66	+ 1.71	1.219
8206.0	+ 0.80	+ 1.85	+ 0.79	+ 1.85	+ 0.79	+ 1.84	+ 0.80	+ 1.85	+ 0.78	+ 1.84	1.219
6251.0	+ 0.34	+ 0.80	+ 0.33	+ 0.80	+ 0.33	+ 0.80	+ 0.34	+ 0.80	+ 0.33	+ 0.79	1.600
5048.0	0.00	0.00	0.00	0.00	0.00	0.00	0.00	0.00	0.00	0.00	1.981
4234.0	- 0.26	- 0.64	- 0.26	- 0.64	- 0.26	- 0.64	- 0.26	- 0.64	- 0.25	- 0.64	2.362
3646.0	- 0.44	- 1.15	- 0.44	- 1.15	- 0.44	- 1.14	- 0.44	- 1.15	- 0.44	- 1.14	2.743
3646.0	+ 0.22	- 0.49	+ 0.23	- 0.48	+ 0.23	- 0.47	+ 0.22	- 0.49	+ 0.24	- 0.46	2.743
2652.0	- 0.00	- 1.40	+ 0.01	- 1.39	+ 0.02	- 1.37	- 0.01	- 1.41	+ 0.03	- 1.36	3.771
2083.0	- 0.13	- 2.05	- 0.11	- 2.04	- 0.09	- 2.01	- 0.15	- 2.08	- 0.09	- 2.01	4.801
1716.0	- 0.21	- 2.55	- 0.19	- 2.53	- 0.16	- 2.50	- 0.25	- 2.60	- 0.17	- 2.51	5.828
1458.0	- 0.26	- 2.96	- 0.24	- 2.93	- 0.20	- 2.89	- 0.32	- 3.01	- 0.22	- 2.92	6.859
1458.0	- 0.26	- 2.96	- 0.24	- 2.93	- 0.20	- 2.89	- 0.32	- 3.01	- 0.22	- 2.92	6.859
1268.0	- 0.29	- 3.29	- 0.26	- 3.26	- 0.21	- 3.21	- 0.36	- 3.36	- 0.25	- 3.25	7.886
1122.0	- 0.30	- 3.56	- 0.26	- 3.53	- 0.21	- 3.48	- 0.38	- 3.65	- 0.26	- 3.52	8.913
1006.0	- 0.30	- 3.80	- 0.27	- 3.77	- 0.21	- 3.71	- 0.40	- 3.90	- 0.26	- 3.76	9.940
911.6	- 0.20	- 3.92	- 0.14	- 3.85	- 0.09	- 3.81	- 0.37	- 4.08	- 0.16	- 3.88	10.970
911.6	+ 8.25	+ 4.53	+ 8.30	+ 4.59	+ 8.40	+ 4.68	+ 8.15	+ 4.43	+ 8.24	+ 4.52	10.970
758.7	+10.68	+ 6.56	+10.76	+ 6.65	+10.90	+ 6.79	+10.51	+ 6.40	+10.63	+ 6.52	13.180
649.4	+13.15	+ 8.69	+13.26	+ 8.81	+13.46	+ 9.01	+12.92	+ 8.46	+13.06	+ 8.61	15.399
567.8	+15.62	+10.88	+15.76	+11.02	+16.03	+11.28	+15.33	+10.59	+15.50	+10.75	17.612
504.3	+18.10	+13.10	+18.26	+13.26	+18.59	+13.59	+17.75	+12.75	+17.94	+12.94	19.829
504.3	+18.14	+13.13	+18.30	+13.29	+18.62	+13.61	+17.80	+12.80	+17.98	+12.97	19.829
387.0	+24.89	+19.32	+25.10	+19.52	+25.53	+19.96	+24.48	+18.91	+24.26	+19.10	25.840
314.0	+31.69	+25.66	+31.91	+25.88	+32.40	+26.37	+31.25	+25.22	+31.46	+25.43	31.847
264.1	+38.56	+32.16	+38.79	+32.39	+39.30	+32.89	+38.11	+31.71	+38.33	+31.92	37.864
228.0	+45.47	+38.75	+45.71	+38.98	+46.22	+39.49	+45.02	+38.29	+45.23	+38.51	43.860

TABLE 3 -- Continued

	Model No. 21		Model No. 22		Model No. 23		Model No. 24		Model No. 25		
λ(Å)	M(1/λ)	M(λ)	M(1/λ)	M(λ)	M(1/λ)	M(λ)	M(1/λ)	M(λ)	M(1/λ)	M(λ)	$1/\lambda(\mu^{-1})$
58350.0	+ 4.54	+ 9.86	+ 4.50	+ 9.82	+ 4.59	+ 9.90	+ 4.59	+ 9.90	+ 4.57	+ 9.88	0.171
29180.0	+ 3.09	+ 6.90	+ 3.05	+ 6.86	+ 3.12	+ 6.93	+ 3.12	+ 6.93	+ 3.11	+ 6.92	0.343
19450.0	+ 2.26	+ 5.19	+ 2.23	+ 5.16	+ 2.30	+ 5.22	+ 2.30	+ 5.23	+ 2.28	+ 5.21	0.514
14590.0	+ 1.69	+ 3.99	+ 1.66	+ 3.97	+ 1.72	+ 4.02	+ 1.72	+ 4.02	+ 1.71	+ 4.01	0.685
14590.0	+ 1.73	+ 4.03	+ 1.70	+ 4.01	+ 1.75	+ 4.06	+ 1.75	+ 4.06	+ 1.74	+ 4.05	0.685
12210.0	+ 1.39	+ 3.30	+ 1.36	+ 3.28	+ 1.41	+ 3.33	+ 1.41	+ 3.33	+ 1.40	+ 3.32	0.819
10500.0	+ 1.10	+ 2.69	+ 1.08	+ 2.67	+ 1.12	+ 2.71	+ 1.12	+ 2.71	+ 1.11	+ 2.70	0.952
9214.0	+ 0.86	+ 2.16	+ 0.84	+ 2.15	+ 0.88	+ 2.18	+ 0.88	+ 2.18	+ 0.87	+ 2.18	1.085
8206.0	+ 0.65	+ 1.70	+ 0.63	+ 1.69	+ 0.67	+ 1.72	+ 0.67	+ 1.72	+ 0.66	+ 1.71	1.219
8206.0	+ 0.78	+ 1.83	+ 0.76	+ 1.82	+ 0.80	+ 1.85	+ 0.79	+ 1.85	+ 0.79	+ 1.84	1.219
6251.0	+ 0.33	+ 0.79	+ 0.32	+ 0.78	+ 0.34	+ 0.80	+ 0.34	+ 0.80	+ 0.33	+ 0.80	1.600
5048.0	0.00	0.00	0.00	0.00	0.00	0.00	0.00	0.00	0.00	0.00	1.981
4234.0	- 0.25	- 0.63	- 0.25	- 0.63	- 0.26	- 0.64	- 0.26	- 0.64	- 0.26	- 0.64	2.362
3646.0	- 0.43	- 1.14	- 0.42	- 1.13	- 0.44	- 1.15	- 0.44	- 1.15	- 0.44	- 1.15	2.743
3646.0	+ 0.26	- 0.45	+ 0.29	- 0.42	+ 0.23	- 0.48	+ 0.23	- 0.48	+ 0.24	- 0.47	2.743
2652.0	+ 0.06	- 1.33	+ 0.12	- 1.28	0.00	- 1.40	0.00	- 1.40	+ 0.02	- 1.38	3.771
2083.0	- 0.05	- 1.97	+ 0.03	- 1.89	- 0.15	- 2.07	- 0.14	- 2.07	- 0.11	- 2.03	4.801
1716.0	- 0.12	- 2.46	- 0.02	- 2.36	- 0.25	- 2.60	- 0.25	- 2.59	- 0.21	- 2.55	5.828
1458.0	- 0.16	- 2.86	- 0.04	- 2.74	- 0.32	- 3.02	- 0.32	- 3.01	- 0.27	- 2.97	6.859
1458.0	- 0.16	- 2.86	- 0.04	- 2.74	- 0.32	- 3.02	- 0.32	- 3.01	- 0.27	- 2.97	6.859
1268.0	- 0.18	- 3.18	- 0.04	- 3.04	- 0.37	- 3.37	- 0.36	- 3.36	- 0.31	- 3.31	7.886
1122.0	- 0.18	- 3.44	- 0.02	- 3.29	- 0.40	- 3.66	- 0.39	- 3.65	- 0.33	- 3.59	8.913
1006.0	- 0.17	- 3.68	0.00	- 3.50	- 0.42	- 3.92	- 0.40	- 3.91	- 0.34	- 3.84	9.940
911.6	- 0.07	- 3.79	+ 0.09	- 3.62	- 0.39	- 4.10	- 0.37	- 4.09	- 0.27	- 3.99	10.970
911.6	+ 8.32	+ 4.60	+ 8.52	+ 4.81	+ 8.10	+ 4.38	+ 8.10	+ 4.39	+ 8.13	+ 4.42	10.970
758.7	+10.74	+ 6.62	+11.03	+ 6.91	+10.43	+ 6.31	+10.43	+ 6.31	+10.46	+ 6.35	13.180
649.4	+13.19	+ 8.74	+13.58	+ 9.13	+12.79	+ 8.34	+12.80	+ 8.34	+12.83	+ 8.38	15.399
567.8	+15.65	+10.91	+16.14	+11.39	+15.17	+10.43	+15.17	+10.43	+15.21	+10.47	17.612
504.3	+18.12	+13.11	+18.69	+13.69	+17.57	+12.56	+17.57	+12.57	+17.61	+12.61	19.829
504.3	+18.15	+13.15	+18.71	+13.70	+17.62	+12.62	+17.62	+12.62	+17.66	+12.66	19.829
387.0	+24.88	+19.30	+25.60	+20.02	+24.27	+18.69	+24.27	+18.69	+24.31	+18.73	25.840
314.0	+31.67	+25.64	+32.45	+26.42	+31.02	+24.99	+31.02	+24.99	+31.06	+25.03	31.847
264.1	+38.54	+32.14	+39.35	+32.94	+37.88	+31.47	+37.88	+31.47	+37.92	+31.51	37.864
228.0	+45.45	+38.73	+46.28	+39.55	+44.78	+38.05	+44.78	+38.06	+44.82	+38.10	43.860

TABLE 3 -- Continued

	Model No. 26		Model No. 27		Model No. 28		Model No. 29		Model No. 30		
λ(Å)	M(1/λ)	M(λ)	M(1/λ)	M(λ)	M(1/λ)	M(λ)	M(1/λ)	M(λ)	M(1/λ)	M(λ)	$1/\lambda(\mu^{-1})$
58350.0	+ 4.53	+ 9.85	+ 4.50	+ 9.81	+ 4.44	+ 9.75	+ 4.49	+ 9.80	+ 4.45	+ 9.76	0.171
29180.0	+ 3.08	+ 6.89	+ 3.05	+ 6.86	+ 2.99	+ 6.80	+ 3.04	+ 6.85	+ 3.00	+ 6.81	0.343
19450.0	+ 2.26	+ 5.19	+ 2.23	+ 5.16	+ 2.18	+ 5.11	+ 2.22	+ 5.15	+ 2.19	+ 5.12	0.514
14590.0	+ 1.68	+ 3.99	+ 1.66	+ 3.97	+ 1.62	+ 3.92	+ 1.65	+ 3.96	+ 1.62	+ 3.93	0.685
14590.0	+ 1.72	+ 4.03	+ 1.70	+ 4.00	+ 1.66	+ 3.96	+ 1.69	+ 4.00	+ 1.67	+ 3.97	0.685
12210.0	+ 1.38	+ 3.30	+ 1.36	+ 3.28	+ 1.32	+ 3.24	+ 1.35	+ 3.27	+ 1.33	+ 3.25	0.819
10500.0	+ 1.10	+ 2.69	+ 1.08	+ 2.67	+ 1.04	+ 2.63	+ 1.07	+ 2.66	+ 1.05	+ 2.64	0.952
9214.0	+ 0.85	+ 2.16	+ 0.84	+ 2.15	+ 0.81	+ 2.11	+ 0.83	+ 2.14	+ 0.81	+ 2.12	1.085
8206.0	+ 0.65	+ 1.70	+ 0.63	+ 1.69	+ 0.60	+ 1.66	+ 0.62	+ 1.68	+ 0.60	+ 1.66	1.219
8206.0	+ 0.77	+ 1.83	+ 0.76	+ 1.82	+ 0.74	+ 1.79	+ 0.76	+ 1.82	+ 0.75	+ 1.80	1.219
6251.0	+ 0.33	+ 0.79	+ 0.32	+ 0.79	+ 0.31	+ 0.77	+ 0.32	+ 0.79	+ 0.31	+ 0.78	1.600
5048.0	0.00	0.00	0.00	0.00	0.00	0.00	0.00	0.00	0.00	0.00	1.981
4234.0	- 0.25	- 0.63	- 0.25	- 0.63	- 0.24	- 0.62	- 0.24	- 0.63	- 0.24	- 0.62	2.362
3646.0	- 0.43	- 1.14	- 0.42	- 1.13	- 0.40	- 1.11	- 0.42	- 1.13	- 0.41	- 1.11	2.743
3646.0	+ 0.26	- 0.44	+ 0.29	- 0.42	+ 0.34	- 0.36	+ 0.30	- 0.41	+ 0.33	- 0.38	2.743
2652.0	+ 0.06	- 1.33	+ 0.11	- 1.28	+ 0.22	- 1.18	+ 0.12	- 1.28	+ 0.18	- 1.22	3.771
2083.0	- 0.05	- 1.98	+ 0.01	- 1.91	+ 0.16	- 1.76	+ 0.01	- 1.91	+ 0.11	- 1.81	4.801
1716.0	- 0.14	- 2.48	- 0.05	- 2.40	+ 0.14	- 2.20	- 0.08	- 2.42	+ 0.06	- 2.28	5.828
1458.0	- 0.19	- 2.88	- 0.09	- 2.78	+ 0.14	- 2.56	- 0.13	- 2.83	+ 0.04	- 2.66	6.859
1458.0	- 0.19	- 2.88	- 0.09	- 2.78	+ 0.14	- 2.56	- 0.13	- 2.83	+ 0.04	- 2.66	6.859
1268.0	- 0.21	- 3.21	- 0.10	- 3.10	+ 0.16	- 2.84	- 0.17	- 3.17	+ 0.03	- 2.97	7.886
1122.0	- 0.22	- 3.49	- 0.10	- 3.36	+ 0.20	- 3.07	- 0.20	- 3.46	+ 0.03	- 3.23	8.913
1006.0	- 0.23	- 3.73	- 0.09	- 3.59	+ 0.24	- 3.26	- 0.22	- 3.72	+ 0.03	- 3.47	9.940
911.6	- 0.13	- 3.85	- 0.01	- 3.72	+ 0.36	- 3.36	- 0.20	- 3.92	+ 0.11	- 3.61	10.970
911.6	+ 8.20	+ 4.49	+ 8.31	+ 4.60	+ 8.64	+ 4.92	+ 8.28	+ 4.57	+ 8.30	+ 4.58	10.970
758.7	+10.54	+ 6.43	+10.67	+ 6.56	+11.11	+ 6.99	+10.54	+ 6.42	+10.55	+ 6.44	13.180
649.4	+12.92	+ 8.47	+13.07	+ 8.62	+13.60	+ 9.14	+12.83	+ 8.38	+12.84	+ 8.39	15.399
567.8	+15.31	+10.57	+15.47	+10.73	+16.08	+11.34	+15.15	+10.40	+15.16	+10.41	17.612
504.3	+17.71	+12.71	+17.89	+12.88	+18.56	+13.56	+17.49	+12.49	+17.51	+12.50	19.829
504.3	+17.76	+12.75	+17.92	+12.92	+18.58	+13.57	+17.56	+12.56	+17.56	+12.55	19.829
387.0	+24.40	+18.83	+24.58	+19.00	+25.32	+19.75	+24.13	+18.56	+24.12	+18.55	25.840
314.0	+31.16	+25.13	+31.34	+25.31	+32.12	+26.09	+30.86	+24.83	+30.85	+24.82	31.847
264.1	+38.02	+31.61	+38.20	+31.79	+38.99	+32.59	+37.71	+31.31	+37.71	+31.30	37.864
228.0	+44.93	+38.20	+45.11	+38.38	+45.91	+39.19	+44.61	+37.89	+44.61	+37.88	43.860

TABLE 3 -- Continued

λ(Å)	Model No. 31		Model No. 32		Model No. 33		Model No. 34		Model No. 35		
	M(1/λ)	M(λ)	M(1/λ)	M(λ)	M(1/λ)	M(λ)	M(1/λ)	M(λ)	M(1/λ)	M(λ)	$1/\lambda(\mu^{-1})$
58350.0	+ 4.39	+ 9.70	+ 4.25	+ 9.56	+ 4.49	+ 9.81	+ 4.48	+ 9.80	+ 4.47	+ 9.79	0.171
29180.0	+ 2.95	+ 6.76	+ 2.83	+ 6.64	+ 3.04	+ 6.85	+ 3.04	+ 6.85	+ 3.02	+ 6.83	0.343
19450.0	+ 2.15	+ 5.07	+ 2.03	+ 4.96	+ 2.22	+ 5.15	+ 2.22	+ 5.15	+ 2.21	+ 5.14	0.514
14590.0	+ 1.58	+ 3.89	+ 1.48	+ 3.78	+ 1.66	+ 3.96	+ 1.65	+ 3.96	+ 1.64	+ 3.95	0.685
14590.0	+ 1.62	+ 3.93	+ 1.52	+ 3.83	+ 1.69	+ 4.00	+ 1.69	+ 3.99	+ 1.68	+ 3.98	0.685
12210.0	+ 1.29	+ 3.21	+ 1.20	+ 3.12	+ 1.36	+ 3.27	+ 1.35	+ 3.27	+ 1.34	+ 3.26	0.819
10500.0	+ 1.01	+ 2.61	+ 0.93	+ 2.52	+ 1.07	+ 2.66	+ 1.07	+ 2.66	+ 1.06	+ 2.65	0.952
9214.0	+ 0.78	+ 2.09	+ 0.71	+ 2.02	+ 0.83	+ 2.14	+ 0.83	+ 2.14	+ 0.82	+ 2.13	1.085
8206.0	+ 0.58	+ 1.63	+ 0.52	+ 1.57	+ 0.63	+ 1.68	+ 0.62	+ 1.68	+ 0.62	+ 1.67	1.219
8206.0	+ 0.72	+ 1.78	+ 0.67	+ 1.72	+ 0.76	+ 1.81	+ 0.76	+ 1.81	+ 0.75	+ 1.81	1.219
6251.0	+ 0.30	+ 0.77	+ 0.27	+ 0.74	+ 0.32	+ 0.78	+ 0.32	+ 0.78	+ 0.32	+ 0.78	1.600
5048.0	0.00	0.00	0.00	0.00	0.00	0.00	0.00	0.00	0.00	0.00	1.981
4234.0	- 0.23	- 0.61	- 0.20	- 0.58	- 0.25	- 0.63	- 0.25	- 0.63	- 0.24	- 0.63	2.362
3646.0	- 0.39	- 1.09	- 0.33	- 1.04	- 0.42	- 1.13	- 0.42	- 1.13	- 0.42	- 1.13	2.743
3646.0	+ 0.37	- 0.34	+ 0.48	- 0.23	+ 0.32	- 0.39	+ 0.32	- 0.38	+ 0.34	- 0.37	2.743
2652.0	+ 0.27	- 1.13	+ 0.55	- 0.85	+ 0.15	- 1.24	+ 0.16	- 1.24	+ 0.18	- 1.22	3.771
2083.0	+ 0.24	- 1.68	+ 0.69	- 1.24	+ 0.06	- 1.86	+ 0.07	- 1.85	+ 0.09	- 1.83	4.801
1716.0	+ 0.23	- 2.11	+ 0.87	- 1.47	0.00	- 2.35	0.00	- 2.34	+ 0.03	- 2.31	5.828
1458.0	+ 0.24	- 2.46	+ 1.07	- 1.63	- 0.03	- 2.73	- 0.03	- 2.73	+ 0.01	- 2.69	6.859
1458.0	+ 0.24	- 2.46	+ 1.07	- 1.63	- 0.03	- 2.73	- 0.03	- 2.73	+ 0.01	- 2.69	6.859
1268.0	+ 0.26	- 2.74	+ 1.28	- 1.72	- 0.05	- 3.05	- 0.05	- 3.05	0.00	- 3.00	7.886
1122.0	+ 0.29	- 2.98	+ 1.50	- 1.76	- 0.04	- 3.31	- 0.04	- 3.31	+ 0.01	- 3.26	8.913
1006.0	+ 0.31	- 3.19	+ 1.71	- 1.79	- 0.03	- 3.53	- 0.03	- 3.54	+ 0.02	- 3.48	9.940
911.6	+ 0.36	- 3.36	+ 1.90	- 1.82	+ 0.17	- 3.54	+ 0.19	- 3.53	+ 0.22	- 3.50	10.970
911.6	+ 8.44	+ 4.72	+ 9.16	+ 5.45	+ 8.97	+ 5.26	+ 9.02	+ 5.31	+ 9.05	+ 5.33	10.970
758.7	+10.69	+ 6.58	+11.48	+ 7.37	+11.65	+ 7.54	+11.70	+ 7.59	+11.73	+ 7.62	13.180
649.4	+12.97	+ 8.52	+13.77	+ 9.31	+14.42	+ 9.96	+14.47	+10.01	+14.50	+10.05	15.399
567.8	+15.28	+10.54	+16.05	+11.31	+17.23	+12.48	+17.28	+12.54	+17.32	+12.57	17.612
504.3	+17.62	+12.62	+18.38	+13.37	+20.09	+15.08	+20.14	+15.13	+20.18	+15.17	19.829
504.3	+17.67	+12.66	+18.40	+13.39	+20.10	+15.10	+20.15	+15.15	+20.19	+15.18	19.829
387.0	+24.22	+18.65	+24.90	+19.33	+28.02	+22.44	+28.06	+22.48	+28.09	+22.52	25.840
314.0	+30.95	+24.92	+31.61	+25.58	+36.07	+30.04	+36.10	+30.07	+36.14	+30.11	31.847
264.1	+37.80	+31.39	+38.46	+32.06	+44.24	+37.83	+44.26	+37.85	+44.29	+37.88	37.864
228.0	+44.71	+37.98	+45.37	+38.65	+52.43	+45.71	+52.44	+45.75	+52.47	+45.74	43.860

TABLE 3 -- Continued

	Model No. 36		Model No. 37		Model No. 38		Model No. 39		Model No. 40		
λ(Å)	M(1/λ)	M(λ)	M(1/λ)	M(λ)	M(1/λ)	M(λ)	M(1/λ)	M(λ)	M(1/λ)	M(λ)	$1/\lambda(\mu^{-1})$
58350.0	+ 4.45	+ 9.77	+ 4.46	+ 9.78	+ 4.42	+ 9.74	+ 4.36	+ 9.67	+ 4.44	+ 9.76	0.171
29180.0	+ 3.01	+ 6.82	+ 3.02	+ 6.83	+ 2.98	+ 6.79	+ 2.92	+ 6.73	+ 3.00	+ 6.81	0.343
19450.0	+ 2.19	+ 5.12	+ 2.20	+ 5.13	+ 2.17	+ 5.10	+ 2.12	+ 5.05	+ 2.18	+ 5.11	0.514
14590.0	+ 1.63	+ 3.93	+ 1.64	+ 3.94	+ 1.61	+ 3.91	+ 1.56	+ 3.87	+ 1.62	+ 3.93	0.685
14590.0	+ 1.67	+ 3.97	+ 1.67	+ 3.98	+ 1.65	+ 3.95	+ 1.60	+ 3.91	+ 1.66	+ 3.97	0.685
12210.0	+ 1.33	+ 3.25	+ 1.34	+ 3.26	+ 1.31	+ 3.23	+ 1.27	+ 3.19	+ 1.33	+ 3.24	0.819
10500.0	+ 1.05	+ 2.64	+ 1.06	+ 2.65	+ 1.03	+ 2.63	+ 1.00	+ 2.59	+ 1.04	+ 2.63	0.952
9214.0	+ 0.82	+ 2.12	+ 0.82	+ 2.13	+ 0.80	+ 2.11	+ 0.77	+ 2.07	+ 0.81	+ 2.12	1.085
8206.0	+ 0.61	+ 1.67	+ 0.61	+ 1.67	+ 0.60	+ 1.65	+ 0.57	+ 1.62	+ 0.60	+ 1.66	1.219
8206.0	+ 0.75	+ 1.80	+ 0.75	+ 1.81	+ 0.74	+ 1.79	+ 0.71	+ 1.77	+ 0.74	+ 1.80	1.219
6251.0	+ 0.31	+ 0.78	+ 0.32	+ 0.78	+ 0.31	+ 0.77	+ 0.30	+ 0.76	+ 0.31	+ 0.78	1.600
5048.0	0.00	0.00	0.00	0.00	0.00	0.00	0.00	0.00	0.00	0.00	1.981
4234.0	- 0.24	- 0.62	- 0.24	- 0.62	- 0.24	- 0.62	- 0.23	- 0.61	- 0.24	- 0.62	2.362
3646.0	- 0.42	- 1.12	- 0.42	- 1.13	- 0.41	- 1.12	- 0.39	- 1.10	- 0.42	- 1.13	2.743
3646.0	+ 0.35	- 0.36	+ 0.34	- 0.36	+ 0.38	- 0.33	+ 0.43	- 0.27	+ 0.36	- 0.35	2.743
2652.0	+ 0.21	- 1.19	+ 0.19	- 1.21	+ 0.26	- 1.14	+ 0.37	- 1.02	+ 0.22	- 1.18	3.771
2083.0	+ 0.13	- 1.79	+ 0.10	- 1.82	+ 0.19	- 1.73	+ 0.36	- 1.56	+ 0.13	- 1.79	4.801
1716.0	+ 0.08	- 2.26	+ 0.03	- 2.32	+ 0.15	- 2.20	+ 0.36	- 1.99	+ 0.06	- 2.28	5.828
1458.0	+ 0.06	- 2.64	- 0.01	- 2.70	+ 0.13	- 2.56	+ 0.38	- 2.31	+ 0.04	- 2.66	6.859
1458.0	+ 0.06	- 2.64	- 0.01	- 2.70	+ 0.13	- 2.56	+ 0.38	- 2.31	+ 0.04	- 2.66	6.859
1268.0	+ 0.06	- 2.94	- 0.02	- 3.02	+ 0.14	- 2.86	+ 0.42	- 2.58	+ 0.03	- 2.97	7.886
1122.0	+ 0.07	- 3.19	- 0.02	- 3.28	+ 0.16	- 3.11	+ 0.48	- 2.79	+ 0.03	- 3.24	8.913
1006.0	+ 0.09	- 3.41	- 0.01	- 3.51	+ 0.18	- 3.32	+ 0.54	- 2.97	+ 0.04	- 3.47	9.940
911.6	+ 0.25	- 3.47	+ 0.30	- 3.41	+ 0.37	- 3.34	+ 0.72	- 3.00	+ 0.43	- 3.29	10.970
911.6	+ 9.08	+ 5.36	+ 9.21	+ 5.49	+ 9.34	+ 5.63	+ 9.58	+ 5.87	+ 9.43	+ 5.71	10.970
758.7	+11.77	+ 7.65	+11.92	+ 7.80	+12.09	+ 7.97	+12.40	+ 8.29	+12.19	+ 8.07	13.180
649.4	+14.54	+10.08	+14.71	+10.25	+14.80	+10.45	+15.29	+10.84	+15.03	+10.57	15.399
567.8	+17.35	+12.61	+17.54	+12.79	+17.76	+13.01	+18.21	+13.46	+17.90	+13.15	17.612
504.3	+20.21	+15.21	+20.41	+15.40	+20.65	+15.65	+21.15	+16.15	+20.80	+15.80	19.829
504.3	+20.22	+15.22	+20.42	+15.42	+20.66	+15.66	+21.16	+16.16	+20.83	+15.83	19.829
387.0	+28.13	+22.55	+28.35	+22.77	+28.62	+23.05	+29.21	+23.64	+28.84	+23.26	25.840
314.0	+36.17	+30.14	+36.40	+30.37	+36.70	+30.67	+37.33	+31.30	+36.95	+30.92	31.847
264.1	+44.32	+37.91	+44.56	+38.15	+44.86	+38.45	+45.51	+39.11	+45.14	+38.74	37.864
228.0	+52.50	+45.77	+52.74	+46.02	+53.05	+46.33	+53.72	+46.99	+53.35	+46.63	43.860

TABLE 3 -- Continued

	Model No. 41		Model No. 42		Model No. 43		Model No. 44		Model No. 45		
λ(Å)	M(1/λ)	M(λ)	M(1/λ)	M(λ)	M(1/λ)	M(λ)	M(1/λ)	M(λ)	M(1/λ)	M(λ)	$1/\lambda(\mu^{-1})$
58350.0	+ 4.39	+ 9.70	+ 4.27	+ 9.59	+ 4.32	+ 9.63	+ 4.27	+ 9.59	+ 4.03	+ 9.34	0.171
29180.0	+ 2.95	+ 6.76	+ 2.85	+ 6.66	+ 2.88	+ 6.69	+ 2.84	+ 6.65	+ 2.62	+ 6.43	0.343
19450.0	+ 2.14	+ 5.07	+ 2.05	+ 4.98	+ 2.08	+ 5.00	+ 2.04	+ 4.97	+ 1.84	+ 4.77	0.514
14590.0	+ 1.58	+ 3.88	+ 1.50	+ 3.81	+ 1.52	+ 3.82	+ 1.48	+ 3.79	+ 1.30	+ 3.60	0.685
14590.0	+ 1.62	+ 3.93	+ 1.54	+ 3.85	+ 1.57	+ 3.87	+ 1.54	+ 3.84	+ 1.36	+ 3.66	0.685
12210.0	+ 1.29	+ 3.21	+ 1.22	+ 3.14	+ 1.24	+ 3.16	+ 1.21	+ 3.13	+ 1.04	+ 2.96	0.819
10500.0	+ 1.01	+ 2.60	+ 0.95	+ 2.54	+ 0.96	+ 2.55	+ 0.94	+ 2.53	+ 0.79	+ 2.38	0.952
9214.0	+ 0.78	+ 2.09	+ 0.72	+ 2.03	+ 0.73	+ 2.04	+ 0.71	+ 2.01	+ 0.57	+ 1.88	1.085
8206.0	+ 0.58	+ 1.63	+ 0.53	+ 1.58	+ 0.53	+ 1.59	+ 0.51	+ 1.57	+ 0.39	+ 1.44	1.219
8206.0	+ 0.72	+ 1.78	+ 0.68	+ 1.74	+ 0.70	+ 1.75	+ 0.68	+ 1.73	+ 0.57	+ 1.63	1.219
6251.0	+ 0.30	+ 0.77	+ 0.28	+ 0.75	+ 0.29	+ 0.75	+ 0.28	+ 0.74	+ 0.22	+ 0.69	1.600
5048.0	0.00	0.00	0.00	0.00	0.00	0.00	0.00	0.00	0.00	0.00	1.981
4234.0	- 0.23	- 0.61	- 0.21	- 0.59	- 0.22	- 0.60	- 0.21	- 0.59	- 0.15	- 0.53	2.362
3646.0	- 0.40	- 1.11	- 0.36	- 1.07	- 0.37	- 1.08	- 0.35	- 1.06	- 0.24	- 0.94	2.743
3646.0	+ 0.41	- 0.29	+ 0.52	- 0.19	+ 0.47	- 0.23	+ 0.52	- 0.19	+ 0.73	+ 0.03	2.743
2652.0	+ 0.32	- 1.08	+ 0.56	- 0.84	+ 0.46	- 0.94	+ 0.58	- 0.82	+ 1.35	- 0.04	3.771
2083.0	+ 0.28	- 1.64	+ 0.64	- 1.28	+ 0.50	- 1.42	+ 0.71	- 1.21	+ 3.21	+ 1.28	4.801
1716.0	+ 0.26	- 2.08	+ 0.74	- 1.60	+ 0.54	- 1.80	+ 0.87	- 1.47	+ 1.96	- 0.38	5.828
1458.0	+ 0.27	- 2.43	+ 0.87	- 1.83	+ 0.62	- 2.07	+ 1.08	- 1.62	+ 1.15	- 1.55	6.859
1458.0	+ 0.27	- 2.43	+ 0.87	- 1.83	+ 0.62	- 2.07	+ 1.08	- 1.62	+ 1.15	- 1.55	6.859
1268.0	+ 0.29	- 2.71	+ 1.00	- 2.00	+ 0.69	- 2.31	+ 1.29	- 1.71	+ 0.79	- 2.21	7.886
1122.0	+ 0.32	- 2.95	+ 1.16	- 2.10	+ 0.75	- 2.51	+ 1.52	- 1.75	+ 0.57	- 2.69	8.913
1006.0	+ 0.36	- 3.15	+ 1.33	- 2.18	+ 0.81	- 2.69	+ 1.73	- 1.77	+ 0.45	- 3.05	9.940
911.6	+ 0.55	- 3.16	+ 1.65	- 2.07	+ 1.74	- 1.98	+ 2.12	- 1.59	+ 0.51	- 3.21	10.970
911.6	+ 9.72	+ 6.01	+10.79	+ 7.08	+12.62	+ 8.90	+11.26	+ 7.55	+ 9.00	+ 5.29	10.970
758.7	+12.59	+ 8.48	+15.05	+10.94	+13.36	+ 9.25	+12.90	+ 8.79	+11.33	+ 7.21	13.180
649.4	+15.54	+11.09	+17.25	+12.80	+15.57	+11.11	+15.23	+10.78	+13.87	+ 9.41	15.399
567.8	+18.53	+13.79	+19.17	+14.43	+18.09	+13.35	+17.80	+13.05	+16.53	+11.78	17.612
504.3	+21.55	+16.55	+21.63	+16.63	+20.79	+15.79	+20.51	+15.51	+19.28	+14.27	19.829
504.3	+21.58	+16.58	+21.63	+16.63	+20.77	+15.76	+20.50	+15.49	+19.28	+14.28	19.829
387.0	+29.90	+24.33	+29.05	+23.48	+28.61	+23.03	+28.32	+22.74	+27.00	+21.43	25.840
314.0	+38.30	+32.27	+36.89	+30.86	+38.25	+32.22	+37.29	+31.26	+34.99	+28.96	31.847
264.1	+46.76	+40.35	+44.93	+38.52	+43.64	+37.23	+43.77	+37.36	+43.23	+36.82	37.864
228.0	+55.21	+48.48	+53.04	+46.32	+50.15	+43.42	+50.18	+43.45	+52.08	+45.35	43.860

TABLE 3 -- Continued

	Model No. 46		Model No. 47		Model No. 48		Model No. 49		
λ(Å)	M(1/λ)	M(λ)	M(1/λ)	M(λ)	M(1/λ)	M(λ)	M(1/λ)	M(λ)	$1/\lambda(\mu^{-1})$
58350.0	+ 4.28	+ 9.60	+ 4.71	+10.03	+ 4.72	+10.03	+ 4.73	+10.04	0.171
29180.0	+ 2.86	+ 6.67	+ 3.24	+ 7.05	+ 3.24	+ 7.05	+ 3.25	+ 7.06	0.343
19450.0	+ 2.06	+ 4.99	+ 2.40	+ 5.33	+ 2.40	+ 5.33	+ 2.40	+ 5.33	0.514
14590.0	+ 1.51	+ 3.81	+ 1.81	+ 4.11	+ 1.81	+ 4.12	+ 1.81	+ 4.12	0.685
14590.0	+ 1.55	+ 3.86	+ 1.84	+ 4.15	+ 1.84	+ 4.15	+ 1.84	+ 4.15	0.685
12210.0	+ 1.23	+ 3.14	+ 1.49	+ 3.41	+ 1.49	+ 3.41	+ 1.49	+ 3.41	0.819
10500.0	+ 0.96	+ 2.55	+ 1.19	+ 2.78	+ 1.19	+ 2.78	+ 1.19	+ 2.78	0.952
9214.0	+ 0.73	+ 2.03	+ 0.94	+ 2.25	+ 0.94	+ 2.25	+ 0.94	+ 2.25	1.085
8206.0	+ 0.53	+ 1.59	+ 0.72	+ 1.78	+ 0.73	+ 1.78	+ 0.73	+ 1.78	1.219
8206.0	+ 0.69	+ 1.74	+ 0.83	+ 1.89	+ 0.83	+ 1.89	+ 0.83	+ 1.88	1.219
6251.0	+ 0.28	+ 0.75	+ 0.35	+ 0.82	+ 0.35	+ 0.82	+ 0.35	+ 0.82	1.600
5048.0	0.00	0.00	0.00	0.00	0.00	0.00	0.00	0.00	1.981
4234.0	- 0.22	- 0.60	- 0.27	- 0.65	- 0.27	- 0.65	- 0.27	- 0.65	2.362
3646.0	- 0.37	- 1.08	- 0.46	- 1.17	- 0.46	- 1.16	- 0.45	- 1.16	2.743
3646.0	+ 0.51	- 0.19	+ 0.08	- 0.63	+ 0.07	- 0.64	+ 0.04	- 0.66	2.743
2652.0	+ 0.54	- 0.86	- 0.21	- 1.61	- 0.22	- 1.62	- 0.25	- 1.65	3.771
2083.0	+ 0.58	- 1.34	- 0.39	- 2.32	- 0.40	- 2.33	- 0.43	- 2.35	4.801
1716.0	+ 0.63	- 1.72	- 0.51	- 2.86	- 0.52	- 2.86	- 0.54	- 2.88	5.828
1458.0	+ 0.69	- 2.00	- 0.59	- 3.29	- 0.60	- 3.29	- 0.60	- 3.29	6.859
1458.0	+ 0.69	- 2.00	- 0.59	- 3.29	- 0.60	- 3.29	- 0.60	- 3.29	6.859
1268.0	+ 0.77	- 2.23	- 0.64	- 3.64	- 0.63	- 3.63	- 0.60	- 3.29	7.886
1122.0	+ 0.86	- 2.41	- 0.66	- 3.93	- 0.64	- 3.90	- 0.59	- 3.86	8.913
1006.0	+ 0.95	- 2.55	- 0.67	- 4.17	- 0.63	- 4.13	- 0.55	- 4.05	9.940
911.6	+ 1.41	- 2.30	- 0.63	- 4.35	- 0.58	- 4.30	- 0.48	- 4.19	10.970
911.6	+10.74	+ 7.02	+ 7.05	+ 3.33	+ 7.06	+ 3.34	+ 7.07	+ 3.35	10.970
758.7	+14.54	+10.42	+ 9.22	+ 5.11	+ 9.23	+ 5.12	+ 9.24	+ 5.13	13.180
649.4	+18.31	+13.85	+11.48	+ 7.02	+11.49	+ 7.03	+11.49	+ 7.04	15.399
567.8	+19.72	+14.97	+13.77	+ 9.03	+13.78	+ 9.04	+13.79	+ 9.04	17.612
504.3	+22.11	+17.11	+16.11	+11.11	+16.12	+11.11	+16.12	+11.11	19.829
504.3	+22.12	+17.12	+16.18	+11.18	+16.19	+11.19	+16.20	+11.20	19.829
387.0	+29.57	+23.99	+22.75	+17.18	+22.76	+17.19	+22.78	+17.20	25.840
314.0	+37.49	+31.46	+29.49	+23.46	+29.50	+23.47	+29.51	+23.48	31.847
264.1	+45.60	+39.20	+36.35	+29.94	+36.36	+29.95	+36.37	+29.96	37.864
228.0	+53.78	+47.06	+43.26	+36.53	+43.27	+36.54	+43.28	+36.56	43.860

energy at any of the thirty-four standard wavelengths. It is these energy distributions that are displayed graphically in Figures 3–9. The last three quantities given in Table 2 are M_v, $(U - B)_0$, and $(B - V)_0$, which all have their standard meaning and are in principle directly observable quantities of unreddened rotating stars of known distance. Additional physical parameters for these same models such as photometric β indices, $V_e \sin i$, the total luminosity, and magnitude of the Balmer jump are found in the more extensive table given by Collins and Harrington (1966).

The one item appearing in Table 2 whose calculation has not been described in detail either in Papers I or II, or by Collins and Harrington (1966), is the absolute visual magnitude M_v. To bring about agreement with Johnson's (1963) zero-age main sequence, we force-fit the appropriate monochromatic flux for the four non-rotating models by means of the expression

$$\text{const.} = \tfrac{1}{4} \sum_{i=1}^{4} (M_{v,i} + 2.5 \log_{10} F_{v,i}), \tag{4}$$

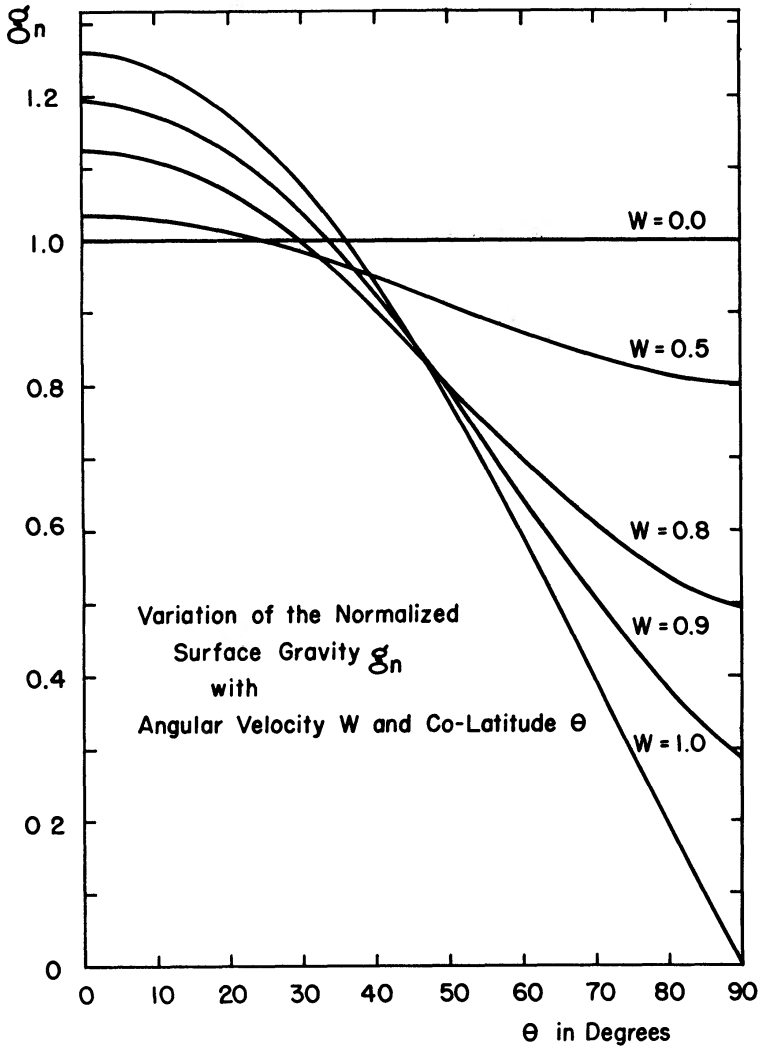

FIG. 1.—Variation of the local surface gravity with changes in w and θ is depicted above. The quantity displayed is the gravity normalized by the non-rotating value.

where the $M_{v,i}$'s are obtained from the Johnson (1963) zero-age main sequence for stars of the appropriate $(B - V)_0$. The standard error in the constant indicates the absolute error in the value of M_v given in Table 2. This turns out to be 0.068 mag. Since this is less than the estimated error of the zero-age main sequence itself, the agreement of all models was thought to be satisfactory. Although the absolute error is moderately large, the relative error is considerably less—on the order of 0.005 mag. Thus, it is possible to invert equation (4) and obtain the absolute visual magnitude for any rotating model:

$$M_v = -2.5 \log F_v + \text{const.} \pm 0.068 . \quad (5)$$

The results of this calculation are shown in Figure 10 as a color-magnitude diagram.

Table 3 contains the detailed results of the calculations in terms of monochromatic magnitudes. The monochromatic magnitudes are given both in wavelength and frequency units at the thirty-four wavelengths specified by the Strömgren-Underhill atmosphere program. The model number at the head of each column of magnitudes allows reference back to Table 2 for the defining parameters of the model.

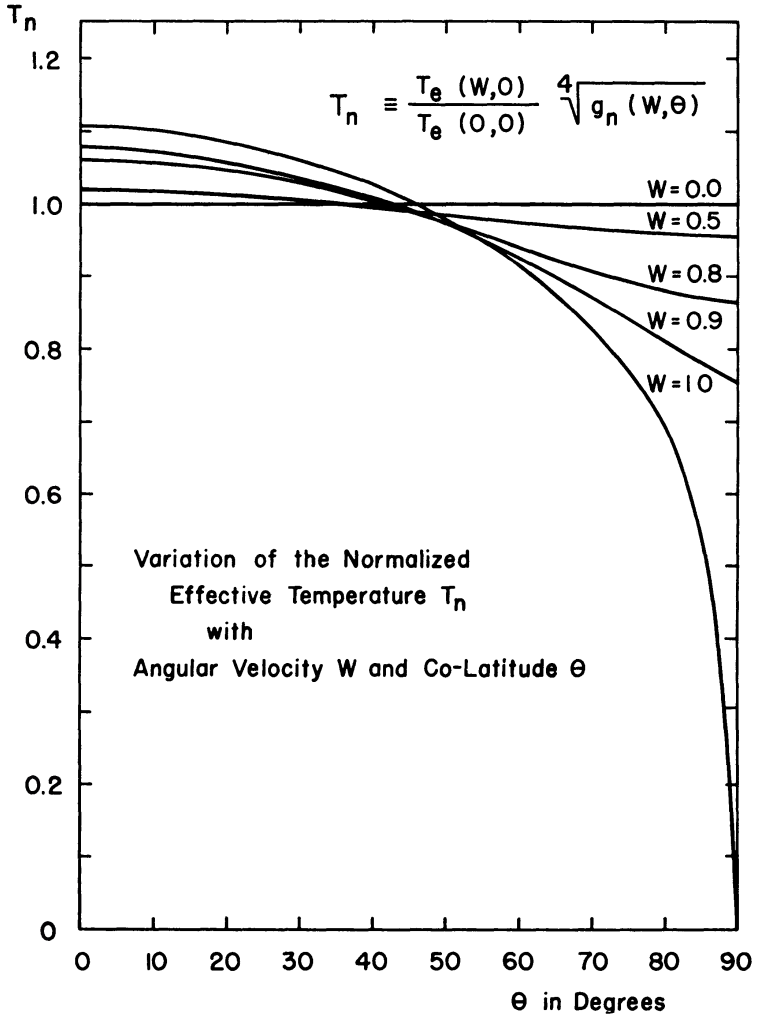

FIG. 2.—Variation of the local effective temperature with changes in w and θ is depicted above. The quantity displayed is the local effective temperature normalized by the non-rotating value.

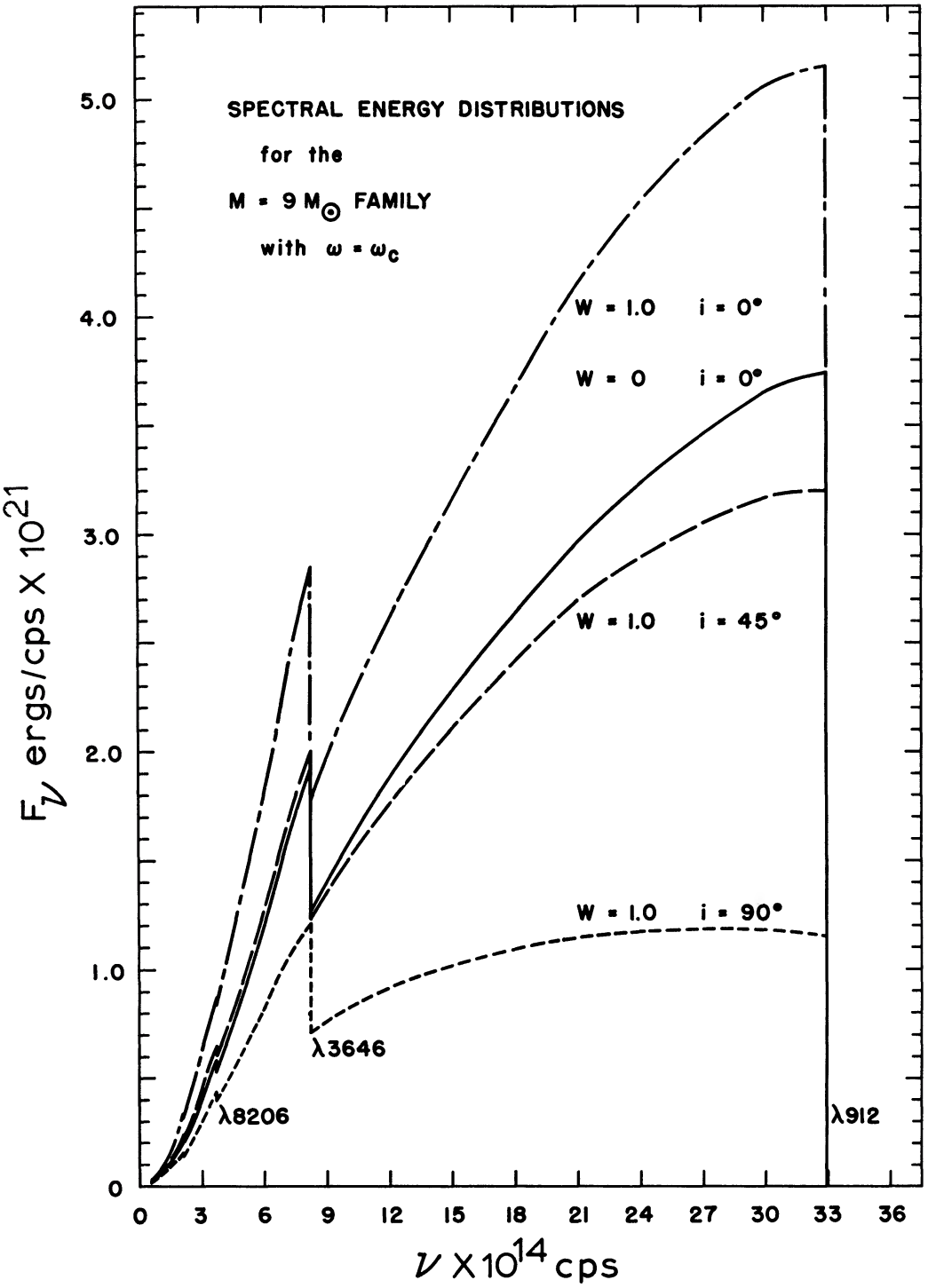

FIG. 3.—Absolute energy distributions for a rotating model with $w = 1.0$ and various angles of inclination. The mass of the model is $M = 9\ M\odot$ and the calculations included limb darkening, gravity darkening, aspect effects, shape distortion, and variation of interior-specified parameters with angular velocity. The solid line in the center of the figure represents the energy distribution for the non-rotating model.

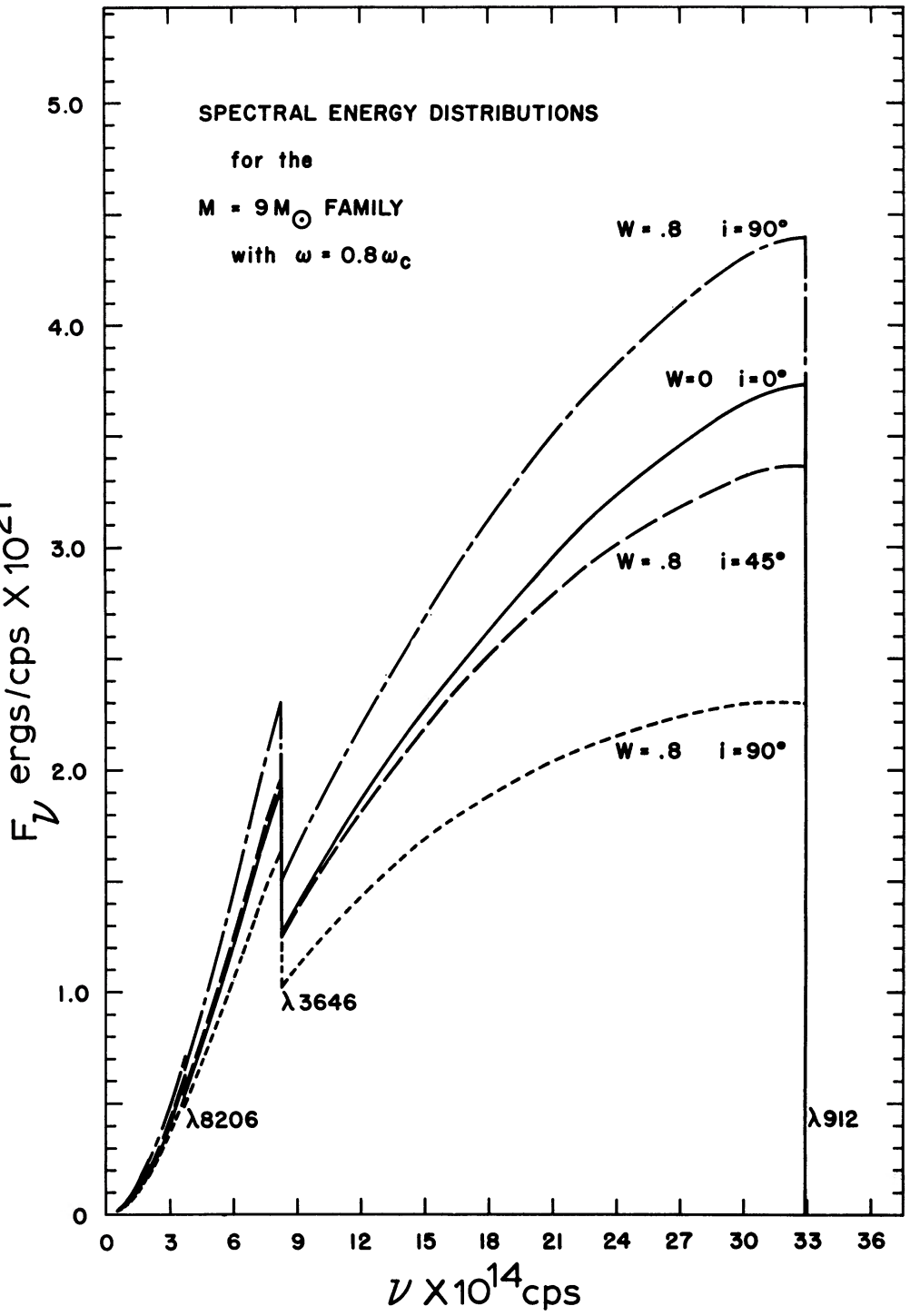

FIG. 4.—Same as Fig. 3, but with $M = 9\ M\odot$ and $w = 0.8$

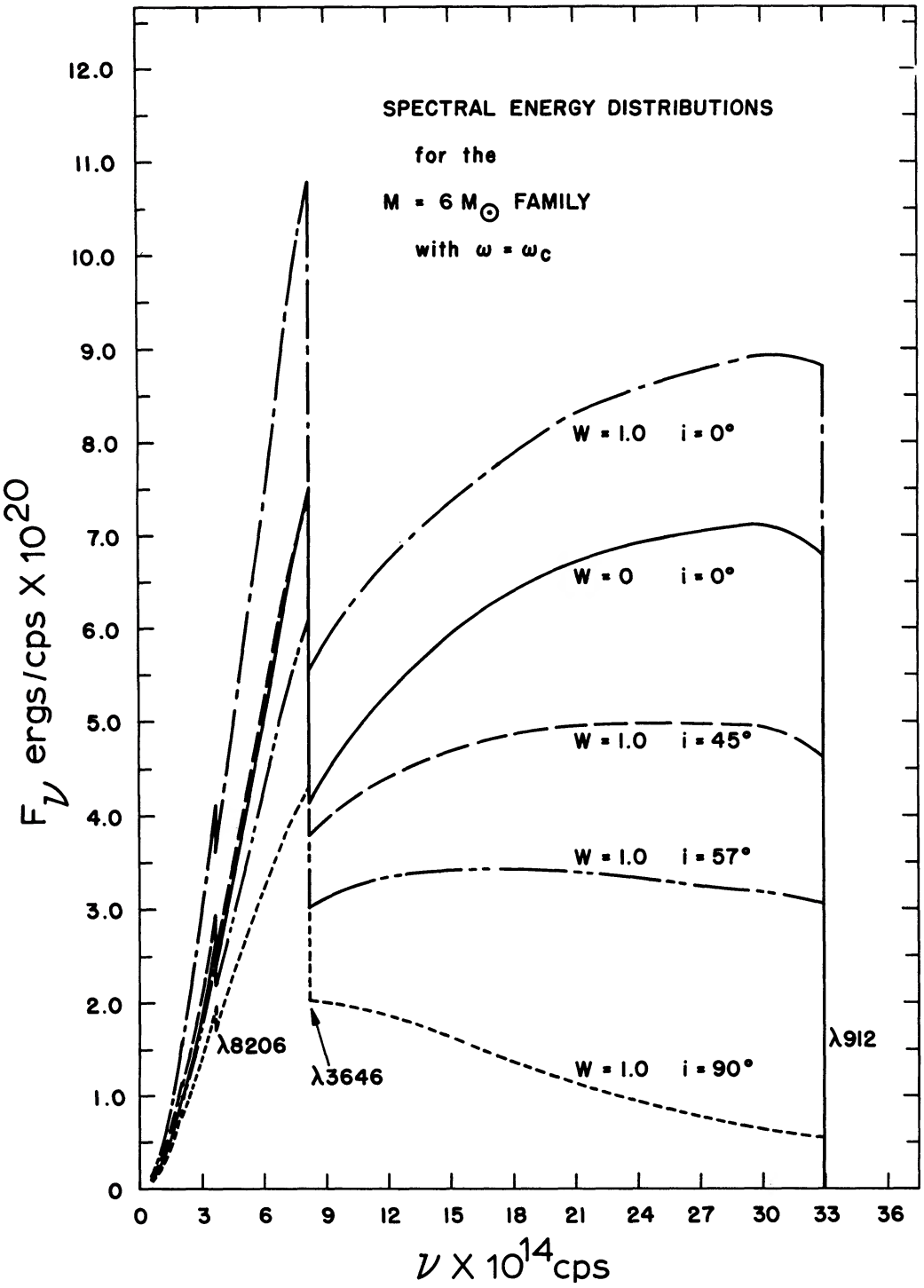

FIG. 5.—Same as Fig. 3, but with $M = 6\ M\odot$ and $w = 1.0$

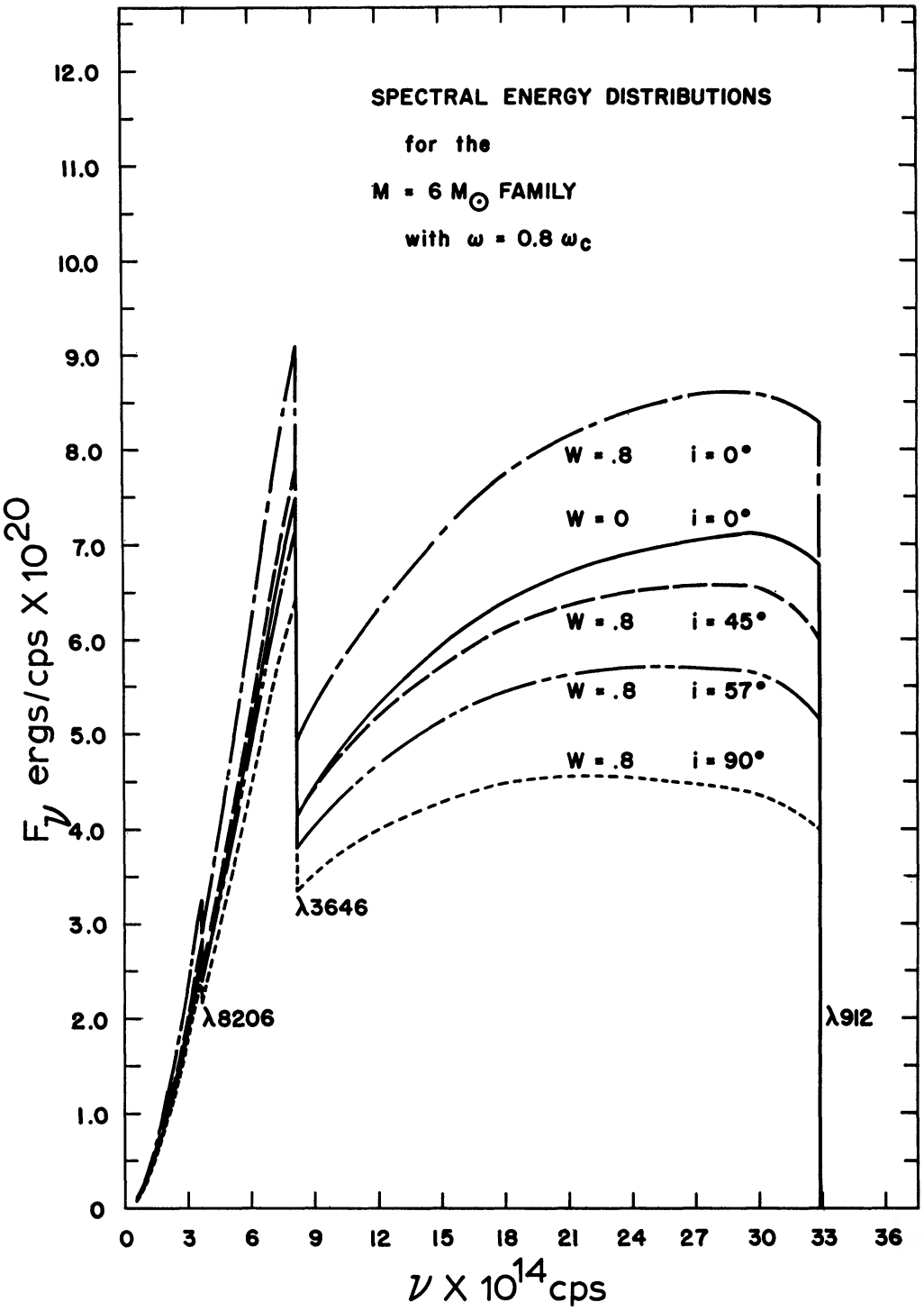

FIG. 6.—Same as Fig. 3, but with $M = 6\ M\odot$ and $w = 0.8$

IV. DISCUSSION OF THE RESULTS

It is instructive to compare the results obtained here with the results obtained in Papers I, II, and the work of Roxburgh and Strittmatter (1965). Paper I and the work of Roxburgh and Strittmatter (1965) both represent computations involving gray-atmosphere approximations and differ only in the assumptions made concerning the variations of the total luminosity and polar radius with angular velocity and in the number of models computed. Except for an error in Paper I, which was subsequently corrected (Collins 1964), the results given for the colors are in satisfactory agreement. This independence of the monochromatic colors on small changes in total luminosity and polar radius was confirmed for the non-gray cases investigated in Paper II and by Collins and Harrington (1966) and was noted in the later work.

However, absolute magnitudes and bolometric magnitudes are quite sensitive to small changes in the total luminosity. For this reason Collins and Harrington (1966) attempted to include variation in both the total luminosity and polar radius within the

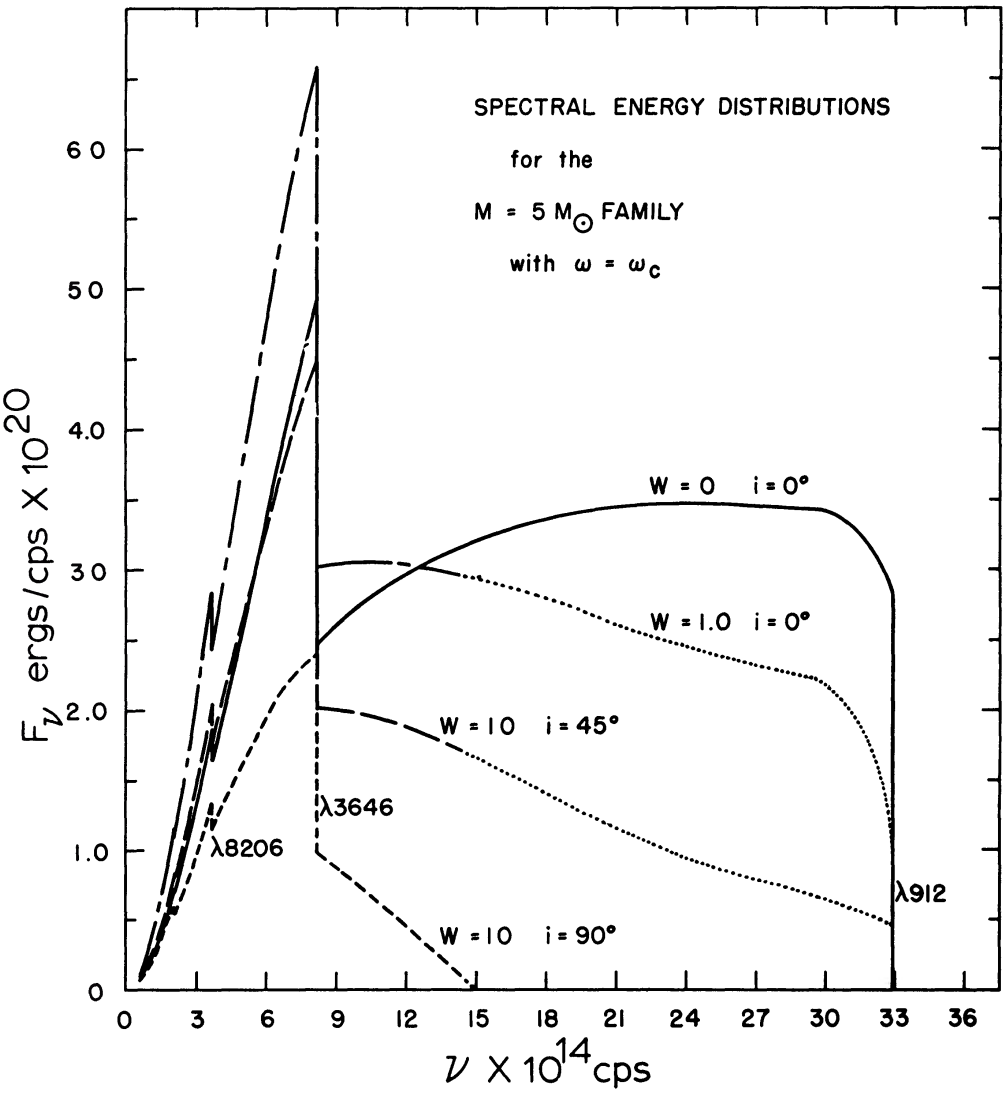

FIG. 7.—Same as Fig. 3, but with $M = 5\ M\odot$ and $w = 1.0$

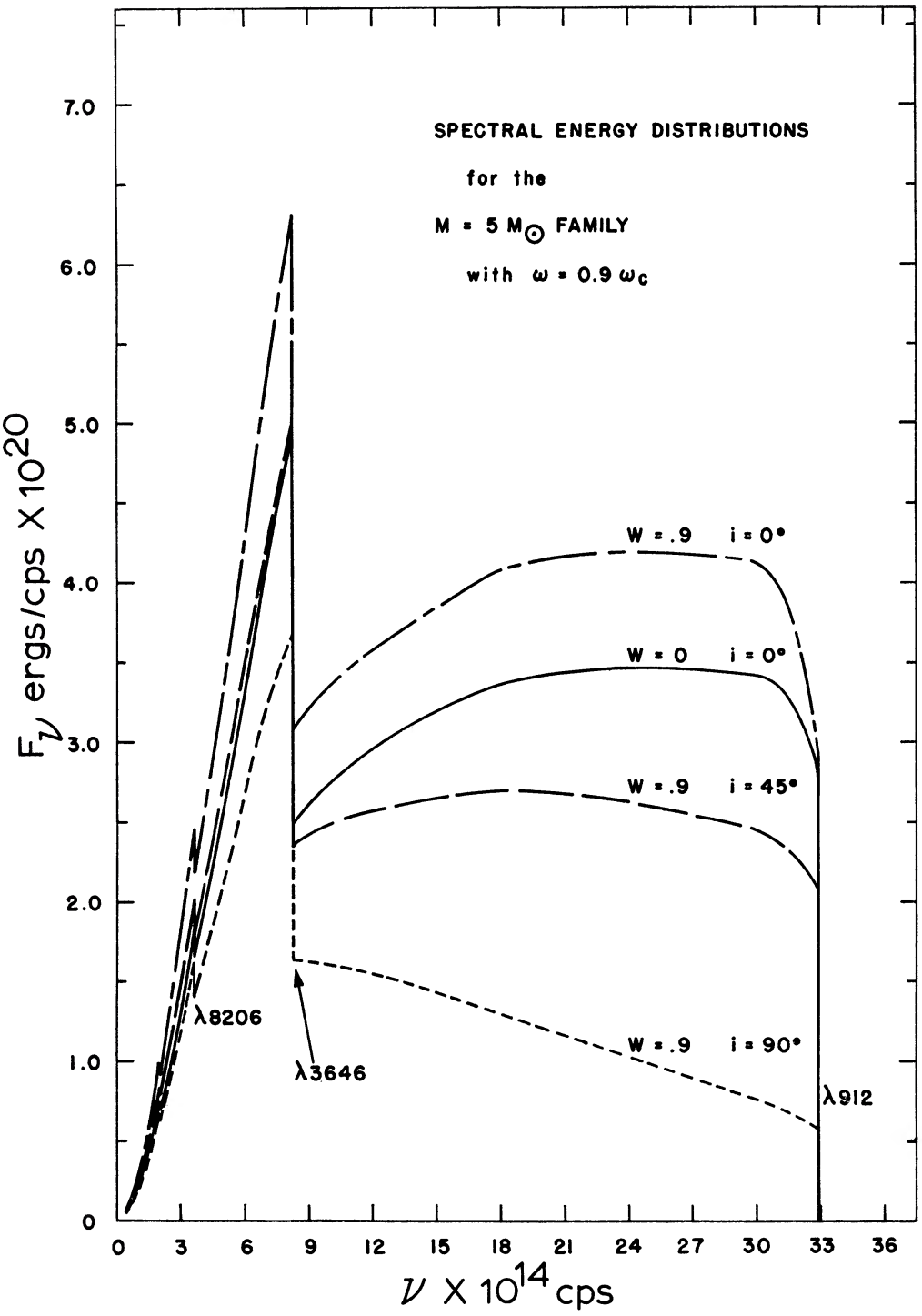

FIG. 8.—Same as Fig. 3, but with $M = 5\ M\odot$ and $w = 0.9$

framework of present theory. The method used by Collins and Harrington (1966) is the one that has been employed in this study and appears to account for the different qualitative behavior of the absolute visual magnitude and bolometric magnitude from that found by Roxburgh and Strittmatter (1965). So that we may understand how these differences arise, it is appropriate that we look at the origin of the expressions used to describe the variation of the total luminosity with angular velocity.

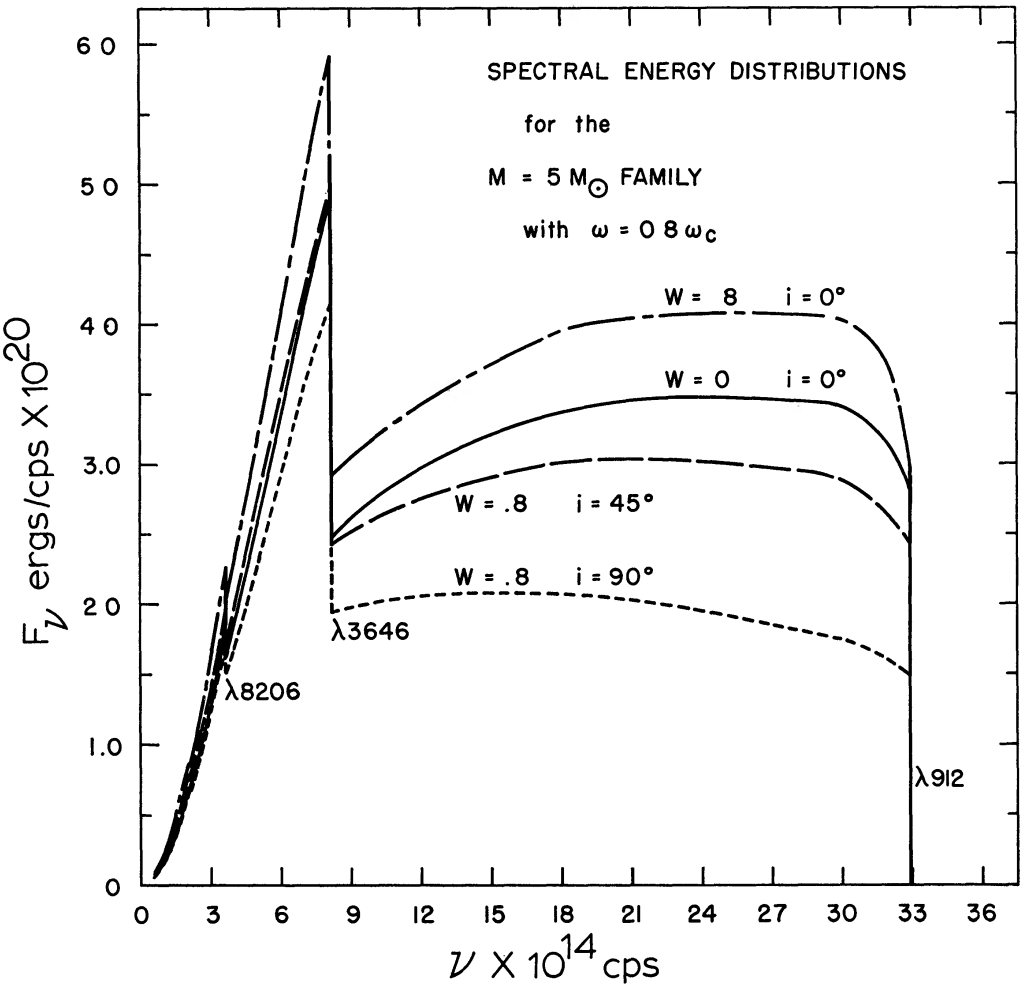

FIG. 9.—Same as Fig. 3, but with $M = 5\ M_{\odot}$ and $w = 0.8$

Sweet and Roy (1953) developed a first-order perturbation theory for the variation of the total luminosity and polar radius. In this theory, the perturbed parameter α was defined as

$$\alpha = w^2/[GM/R_p^3(0)]\,, \tag{6}$$

which may be expressed in terms of our parameter w by

$$\alpha = w^2[R(\text{non-rot.})/R_e(\text{breakup})]^3\,. \tag{7}$$

Roxburgh *et al.* (1965) gave a value of 1.337 for the ratio of the equatorial radius of a star for which $w = 1.0$, to the radius of a non-rotating star. Combining this with the

formulae given by Sweet and Roy (1953), we find that the appropriate first-order theory for Roxburgh-type model interiors would yield

$$L(w) = L(0)(1 - 0.1678\, w^2), \qquad R_p(w) = R_p(0)(1 - 0.0540\, w^2)\,. \tag{8}$$

However, Sweet and Roy (1953) noted that the theory would break down for the higher rotational velocities and that a higher-order perturbation theory was required. Collins and Harrington (1966) attempted to estimate the effects of the higher-order terms that a better perturbation theory would develop by using the breakup model of Roxburgh *et al.* to estimate the second-order term in a. This leads to the expressions given by them and repeated here in equations (1). These expressions have the desirable properties of agreeing with the Sweet and Roy (1953) theory for small w and agreeing with the Roxburgh *et al.* model for large w.

The expressions given by Roxburgh and Strittmatter (1965) may be obtained by

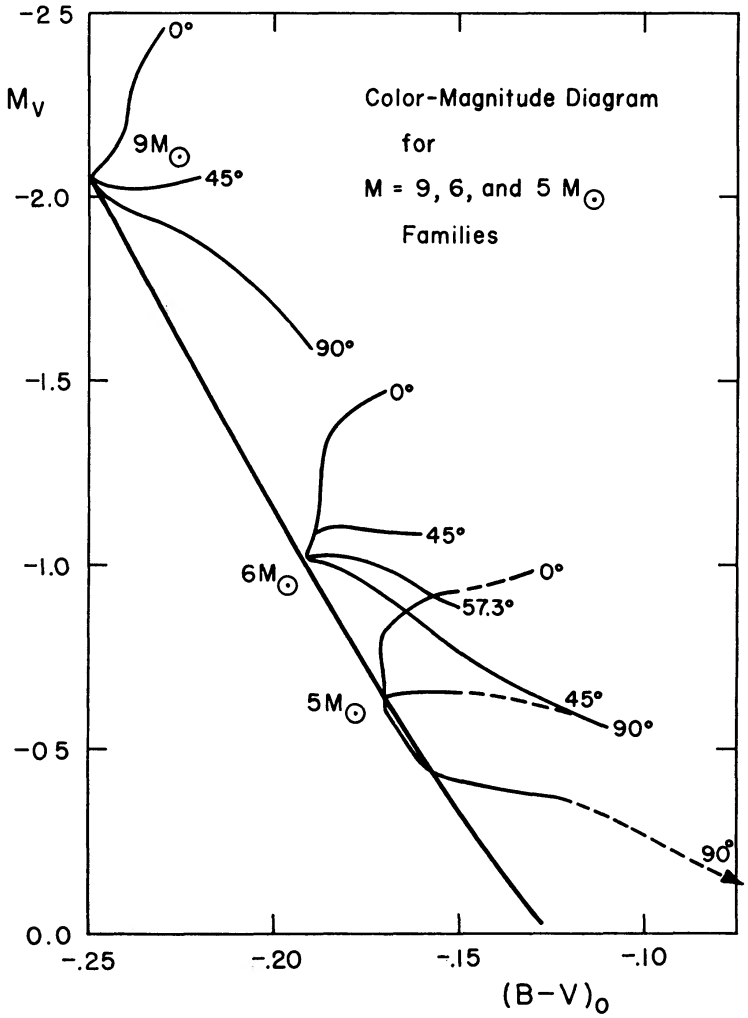

FIG. 10.—Color-magnitude diagram for the three families of models with M = 9, 6, and 5 $M_\odot$. The various tracks for a given family represent different angles of inclination. A given model moves out along these tracks as a higher angular velocity is selected The solid diagonal line is the Johnson zero-age main sequence.

using the Roxburgh *et al.* model to determine the first-order term in a (i.e., w^2). This leads to the expressions

$$L(w) = L(0)(1 - 0.247\ w^2), \qquad R_p(w) = R_p(0)(1 - 0.1087\ w^2)\,, \tag{9}$$

which are in conflict with the Sweet and Roy (1953) first-order theory for small values of w. As a result Roxburgh and Strittmatter (1965) overestimate the correction terms for the total luminosity and polar radius by about 50 per cent for small and moderate values of w. Correction of the results of Roxburgh and Strittmatter (1965) by an amount given by the ratio of equations (1)–(9) bring about qualitative agreement between these results and this paper.

The fact that, even after correction of the results for variations of $L(w)$ and $R_p(w)$, there still remains a quantitative difference in the colors and magnitudes most probably results from the different type of atmospheres used. Collins (1965) demonstrated that using non-gray rather than gray atmospheres to determine the radiation field tended to enhance the effects of rotation over those found in a gray atmosphere study. Thus, it is not surprising that we should find that changes in the absolute magnitude are as much as 0.2 to 0.5 mag. larger than those found by Roxburgh and Strittmatter (1965). Also, changes in the colors $(B - V)_0$ are somewhat larger than those found by Roxburgh and Strittmatter (1965) or in Paper I.

It is interesting to contemplate the extent to which these results will be useful in determining the rotational properties of stars. Kraft and Wrubel (1965) have found a correlation between the C_1 and the observed $V \sin i$. Strittmatter (1966) has looked for relationships between expected changes in M_v with rotation and $V \sin i$. The success of these investigations has been, in part, due to the fact that they have to a large extent been restricted to A- and later-type stars. In this region the main sequence is fairly narrow and the effects of rotation on the visible part of the spectrum is quite large even for moderate rotation. In addition, the rotation encountered in these stars is not very great. Thus, we could expect the first-order theory of Sweet and Roy (1953) to give good results.

However, for stars of spectral type B, the rotational effects in the visible region are smaller than for the A stars with a corresponding w. In addition, the cosmic scatter of the main sequence is considerably larger. This scatter may in part result from such effects as rotation and evolution and perhaps even abundance differences. Even though, as is illustrated by Figure 10, rotation causes stars to lie to the left of the zero-age main sequence it is unlikely that this fact alone is sufficient to separate rapidly rotating stars from slowly rotating ones. For those stars the linear theory is no longer applicable and thus $\Delta_0 M_v$ (the change in the absolute magnitude at a given color) is not simply proportional to V^2, but also depends on $V \sin i$. Collins and Harrington (1966) have already shown that the effect on a color-color diagram is such as not to be directly useful in determining the effects of rotation. Thus, it would appear that only through the combined effects of rotation upon the continuum and upon line strengths will it be possible to accurately investigate the phenomenon of rotation in B stars. The author is currently investigating the effects of rotation upon the continuum and line strengths of Hβ and Hγ as evidenced in stars found in young clusters and OB associations.

Continuing thanks and gratitude are due Dr. Roy Reeves and the staff of the Ohio State University Computation Center for making available the computating facilities and time required for this study.

REFERENCES

Collins, G. W., II. 1963, *Ap. J.*, **138**, 1134 (Paper I).
———. 1964, *ibid.*, **139**, 1401.
———. 1965, *ibid.*, **142**, 265 (Paper II).

Collins, G. W., II, and Harrington, J. P. 1966, *Ap. J.*, **146,** 152 (Paper II).
Johnson, H. L. 1963, *Basic Astronomical Data* (Chicago: University of Chicago Press), p. 204.
Kraft, R. P., and Wrubel, M. 1965, *Ap. J.*, **142,** 703.
Limber, D. N., and Roberts, P. H. 1965, *Ap. J.*, **141,** 1439.
Roxburgh, I. W., Griffith, J. S., and Sweet, P. A. 1965, *Z. f. Ap.*, **61,** 203.
Roxburgh, I. W., and Strittmatter, P. A. 1965, *Z. f. Ap.*, **63,** 15.
Strittmatter, P. A. 1966, *Ap J.*, **144,** 430.
Sweet, P. A., and Roy, A. E. 1953, *M.N.*, **113,** 701.